

Type IIA Orientifolds on General Supersymmetric \mathbb{Z}_N Orbifolds

Ralph Blumenhagen,¹ Joseph P. Conlon² and Kerim Suruliz³

*DAMTP, Centre for Mathematical Sciences,
Wilberforce Road, Cambridge, CB3 0WA, UK*

Abstract

We construct Type IIA orientifolds for general supersymmetric \mathbb{Z}_N orbifolds. In particular, we provide the methods to deal with the non-factorisable six-dimensional tori for the cases \mathbb{Z}_7 , \mathbb{Z}_8 , \mathbb{Z}'_8 , \mathbb{Z}_{12} and \mathbb{Z}'_{12} . As an application of these methods we explicitly construct many new orientifold models.

¹e-mail: R.Blumenhagen@damtp.cam.ac.uk

²e-mail: J.P.Conlon@damtp.cam.ac.uk

³e-mail: K.Suruliz@damtp.cam.ac.uk

Contents

1	Introduction	2
2	Type IIA orientifolds on non-factorisable orbifolds	4
2.1	Definition of ΩR orientifolds	4
2.2	Dealing with non-factorisable lattices	9
3	The massless spectrum	12
3.1	The closed string spectrum	12
3.2	The open string spectrum	13
4	Examples of factorisable orientifolds revisited	14
5	Examples of non-factorisable orientifolds	15
5.1	\mathbb{Z}_7 Model : A_7 with $v = \frac{1}{7}(1, 2, -3)$	15
5.2	\mathbb{Z}'_8 Model: $B_2 \times B_4$ with $v = \frac{1}{8}(2, 1, -3)$	20
5.3	\mathbb{Z}_8 Model: $D_2 \times B_4$ with $v = \frac{1}{8}(-4, 1, 3)$	25
5.4	\mathbb{Z}_{12} Model: $A_2 \times F_4$ with $v = \frac{1}{12}(4, 1, -5)$	26
5.5	\mathbb{Z}'_{12} Model: $D_2 \times F_4$ with $v = \frac{1}{12}(-6, 1, 5)$	28
5.6	\mathbb{Z}_4 Model: $A_3 \times A_3$ with $v = \frac{1}{4}(1, -2, 1)$	29
6	Conclusions	34
A	Oscillator Formulae	36
B	Lattices	38

1 Introduction

The last years have seen some considerable effort in constructing new string vacua with D-branes in the background. The natural set-up involves so-called orientifold models, for which tadpole cancellation really forces us to introduce D-branes, which from the low energy point of view extends the closed string gravity theory by gauge degrees of freedom (see [1] and refs. therein). Therefore, besides the heterotic string these orientifold models constitute a class of string backgrounds which exhibit interesting phenomenological properties.

It is by now well established that chirality can be implemented in Type IIA orientifold models by using intersecting D6-branes, where each topological intersection point gives rise to a chiral fermion. Indeed, following some earlier work [2, 3, 4, 5, 6, 7, 8, 9, 10, 11] many of these so-called intersecting D-brane models have been constructed so far, which feature some of the properties of the non-supersymmetric [12, 13, 14, 15, 16, 17, 18] or supersymmetric Standard Model

[19, 20, 21, 22, 23, 24, 25, 26, 27] (please consult the reviews [28, 29] for more refs.).

However, the class of closed string backgrounds studied so far is still quite limited. There are two principal classes of models which are still under investigation. One is the class of toroidal orbifold backgrounds, for which only a limited number of examples have been investigated so far [19, 20, 21, 22, 25, 26]. The second class are orientifolds of Gepner models [30, 31], for which the general structure of the one-loop amplitudes and the tadpole cancellation conditions were worked out recently in [32, 33, 34, 35, 36, 37, 38].

The aim of this paper is to extend the work on Type IIA orientifolds of toroidal orbifolds, where so far only the cases $\mathbb{Z}_2 \times \mathbb{Z}_2$, \mathbb{Z}_3 , \mathbb{Z}_4 , $\mathbb{Z}_4 \times \mathbb{Z}_2$ and \mathbb{Z}_6 have been studied to the extent that chiral intersecting D6-brane models have been constructed. The main reason for focusing on these orbifolds is of technical nature, namely that in these cases the complex structure of the six-dimensional torus can be chosen such that it decomposes as $T^6 = T^2 \times T^2 \times T^2$. All the other \mathbb{Z}_N Type IIA orientifolds, namely \mathbb{Z}_7 , \mathbb{Z}_8 , \mathbb{Z}'_8 , \mathbb{Z}_{12} and \mathbb{Z}'_{12} , are not completely factorisable in the above sense and so far remained largely unexplored. It is the aim of this paper to resolve some of the technical problems with describing these orientifolds properly and to provide the necessary technical tools.

Note, that Type IIB orientifolds on these non-factorisable orbifolds are technically much simpler and partition functions could be computed fairly straightforwardly [39, 40]. However, it was found there that certain Type IIB \mathbb{Z}_N orientifolds with N even do not allow for tadpole cancelling configurations of $D9$ and $D5$ branes [41, 40, 42]. We would like to point out that first the Type IIA models considered here are not T-dual to the Type IIB models mentioned above and second that in our case we always find tadpole cancelling configurations. This is surely related to the fact that here only untwisted and almost trivial \mathbb{Z}_2 twisted sector tadpoles appear, whereas in the Type IIB case twisted tadpoles in all sectors do arise.

Of course we are finally interested in constructing chiral supersymmetric intersecting brane models on these non-factorisable orbifolds. After determining the general form of the Klein-bottle amplitudes, as a starting point we restrict ourselves to the solutions with D6-branes placed on top of the orientifold planes, thus generalising the work of [6, 7, 8]. As we will discuss, to construct these solutions properly, some new ingredients in the computation of the one-loop amplitudes need to be employed.

This paper is organised as follows. In section 2 we first review the classification of supersymmetric \mathbb{Z}_N orbifolds allowing for a crystallographic action of the symmetry. Then we provide the general framework to deal with the non-factorisable orbifolds and derive general results for the various one-loop amplitudes. Section 3 contains the rules for computing both the closed and the open string spectrum. In section 4 we revisit and extend the factorisable orbifolds studied already in [6]. In section 5 we apply our techniques to the construction of new orientifolds on

non-factorisable orientifolds, where we discuss quite a large number in detail and encounter some new technical subtleties in computing the one-loop amplitudes. As a first step, here we focus on the non-chiral solutions to the tadpole cancellation conditions with D6-branes right on top of the orientifold planes. Finally, section 6 contains our conclusions.

2 Type IIA orientifolds on non-factorisable orbifolds

In this section we first review some facts about ΩR orientifolds and the classification of supersymmetric six-dimensional orbifolds. In the second part we develop new methods to deal with the non-factorisable lattices and to compute one-loop partition functions from which one can extract the tadpole cancellation conditions.

2.1 Definition of ΩR orientifolds

Orientifolds are a natural method for introducing D-branes into a theory. Suppose we start with type II string theory on a background $\mathbb{M}^4 \times X_6$, where for our purposes X_6 will be assumed compact. An orientifold is defined by taking the quotient of this theory by $H = F + \Omega G$, where F and G are discrete groups of target space symmetries. If G were empty, we would have an orbifold - the orientifold is defined by the fact that the symmetry we divide out by involves worldsheet orientation reversal Ω . We then project onto states that are invariant under this symmetry.

The fixed points of G define an O-plane. These are non-dynamical, geometric surfaces that carry R-R charge and have a nonzero tadpole amplitude to emit closed strings into the bulk. Unoriented closed string theories are generally inconsistent due to this uncanceled R-R charge located on the O-planes. In the compact space X_6 , the R-R flux has nowhere to escape to and it is necessary to add D-branes to cancel the overall R-R charge. Closed strings then couple to both D-branes and O-planes, each giving a tadpole amplitude for the emission of closed strings into the vacuum. The disc (D-brane) and \mathbb{RP}_2 (O-plane) tadpoles give rise to infrared divergences due to closed string exchange in the one-loop diagrams. This can be computed as a tree channel diagram, by constructing boundary and crosscap states and finding their overlap (for a review see [43]). However, world-sheet duality means that we can reinterpret closed string tree channel diagrams as open string or closed string one loop diagrams. In this paper we are not making explicit use of the tree channel approach, but instead start directly with the computation of the relevant loop channel amplitudes, i.e. the Klein bottle, annulus and Möbius strip amplitude.

Table 1: Possible orbifold actions preserving N=1 supersymmetry

\mathbb{Z}_3	$(1, 1, -2)/3$	\mathbb{Z}_4	$(1, 1, -2)/4$	\mathbb{Z}_6	$(1, 1, -2)/6$
\mathbb{Z}'_6	$(1, 2, -3)/6$	\mathbb{Z}_7	$(1, 2, -3)/7$	\mathbb{Z}_8	$(1, 3, -4)/8$
\mathbb{Z}'_8	$(2, 1, -3)/8$	\mathbb{Z}_{12}	$(4, 1, -5)/12$	\mathbb{Z}'_{12}	$(-6, 1, 5)/12$

In this paper we will consider what are called ΩR orientifolds. The group G always includes the element R , which acts as

$$R : Z_i \leftrightarrow \bar{Z}_i \quad i = 1, 2, 3 \quad (1)$$

on the complex coordinates $Z_1 = x_4 + ix_5$, $Z_2 = x_6 + ix_7$, $Z_3 = x_8 + ix_9$. The action of ΩR on R-R states is then

$$\Omega R |s_0, s_1, s_2, s_3\rangle \otimes |s'_0, s'_1, s'_2, s'_3\rangle = -|s'_0, -s'_1, -s'_2, -s'_3\rangle \otimes |s_0, -s_1, -s_2, -s_3\rangle \quad (2)$$

and consequently ΩR is, for four-dimensional compactifications, a symmetry of type IIA string theory. Note that for the analogous six-dimensional case ΩR is a symmetry of type IIB.

The models we consider are ΩR orientifolds of type IIA orbifolds. It was shown in the mid eighties [44, 45] that all orbifold actions Θ satisfying modular invariance and preserving 4-dimensional $N = 2$ supersymmetry can be written as

$$\begin{aligned} Z_i &\rightarrow \exp(2\pi i v_i) Z_i \\ \bar{Z}_i &\rightarrow \exp(-2\pi i v_i) \bar{Z}_i \end{aligned} \quad (3)$$

where v_i has the possible values given in table 1.

The requirement that Θ act crystallographically places stringent conditions on the compact space X_6 , namely X_6 must be a toroidal lattice and in fact there are only 18 distinct possibilities [46]. These are listed in table 2 together with the corresponding numbers of $(1, 1)$ and $(1, 2)$ -forms, $h^{1,1}$ and $h^{1,2}$. For 15 of these cases, the orbifold action can be realised as the Coxeter element $\omega = \Gamma_1 \Gamma_2 \Gamma_3 \Gamma_4 \Gamma_5 \Gamma_6$ acting on the root lattice of an appropriate Lie algebra. For the other three, the orbifold action is instead realised as a combination of Weyl reflections and outer automorphisms acting on the Lie algebra root lattice. This is shown in the last column of table 2. Γ_i is a Weyl reflection on the simple root i and P_{ij} exchanges roots i and j . For most of the orbifolds in this paper, and for all those we study in detail, there is no distinction between the orbifold action Θ and the Coxeter element ω . However, notationally we will tend to use Θ when referring to an element of the orbifold group and ω when referring to its action on the basis vectors of the lattice. We trust this will not cause confusion.

So far ΩR orientifolds have only been constructed for a few of the orbifolds in table 2. To construct the orientifold, ΩR must be a well-defined symmetry of the

Table 2: The 18 symmetric \mathbb{Z}_N orbifolds

Case	Lie algebra root lattice	$h^{1,1}$	$h^{1,2}$	Orbifold action Θ
1 \mathbb{Z}_3	$A_2 \times A_2 \times A_2$	36	-	ω
2 \mathbb{Z}_4	$A_1 \times A_1 \times B_2 \times B_2$	31	7	ω
3 \mathbb{Z}_4	$A_1 \times A_3 \times B_2$	27	3	ω
4 \mathbb{Z}_4	$A_3 \times A_3$	25	1	ω
5 \mathbb{Z}_6	$A_2 \times G_2 \times G_2$	29	5	ω
6 \mathbb{Z}_6	$G_2 \times A_2 \times A_2$	25	1	$\Gamma_1 \Gamma_2 \Gamma_3 \Gamma_4 P_{36} P_{45}$
7 \mathbb{Z}'_6	$A_1 \times A_1 \times A_2 \times G_2$	35	11	ω
8 \mathbb{Z}'_6	$A_2 \times D_4$	29	5	ω
9 \mathbb{Z}'_6	$A_1 \times A_1 \times A_2 \times A_2$	31	7	$\Gamma_1 \Gamma_2 \Gamma_3 \Gamma_4 P_{36} P_{45}$
10 \mathbb{Z}'_6	$A_1 \times A_5$	25	1	ω
11 \mathbb{Z}_7	A_6	24	-	ω
12 \mathbb{Z}_8	$B_4 \times D_2$	31	7	ω
13 \mathbb{Z}_8	$A_1 \times D_5$	27	3	ω
14 \mathbb{Z}'_8	$B_2 \times B_4$	27	3	ω
15 \mathbb{Z}'_8	$A_3 \times A_3$	24	-	$\Gamma_1 \Gamma_2 \Gamma_3 P_{16} P_{25} P_{34}$
16 \mathbb{Z}_{12}	$A_2 \times F_4$	29	5	ω
17 \mathbb{Z}_{12}	E_6	25	1	ω
18 \mathbb{Z}'_{12}	$D_2 \times F_4$	31	7	ω

theory and thus R must act crystallographically on the lattice. The cases 1,2,5 and 7 were first studied in [6] and have lattices factorisable as $T^2 \times T^2 \times T^2$. For these cases, the action of R is found more or less by inspection. However, the generic lattice is non-factorisable and it is not obvious how to visualise it.

To study the other cases in table 2 we need to find a crystallographic implementation of R . The rotation planes of the orbifold action ω are orthogonal. If we take a given lattice vector, we can decompose it into components lying in each of the orbifold rotation planes. On each component, ω acts as a pure rotation. We choose one lattice vector, \mathbf{e}_1 , of minimal size. For convenience, we orient the rotation planes such that \mathbf{e}_1 lies along the x -axis in each plane. As ω acts crystallographically, $\omega \mathbf{e}_1$ is also a lattice vector. Repeated action of ω generates a basis of lattice vectors. It is necessary to check that this is actually a basis for the lattice; in practice this is ensured by requiring \mathbf{e}_1 to be of minimal size. Then, if $\omega^N = 1$,

$$R : \omega^k \mathbf{e}_i \leftrightarrow \omega^{N-k} \mathbf{e}_i \quad (4)$$

and is manifestly crystallographic. As an illustration of this construction, in figure 1 the lattice vectors are shown for the \mathbb{Z}_{12} case, where the Lie algebra is $A_2 \times F_4$ and the orbifold rotation $v = \frac{1}{12}(4, 1, -5)$.

Table 2 lists the Lie algebras on whose root lattices the orbifold action is implemented. However, we are not interested in the root structure of the algebra

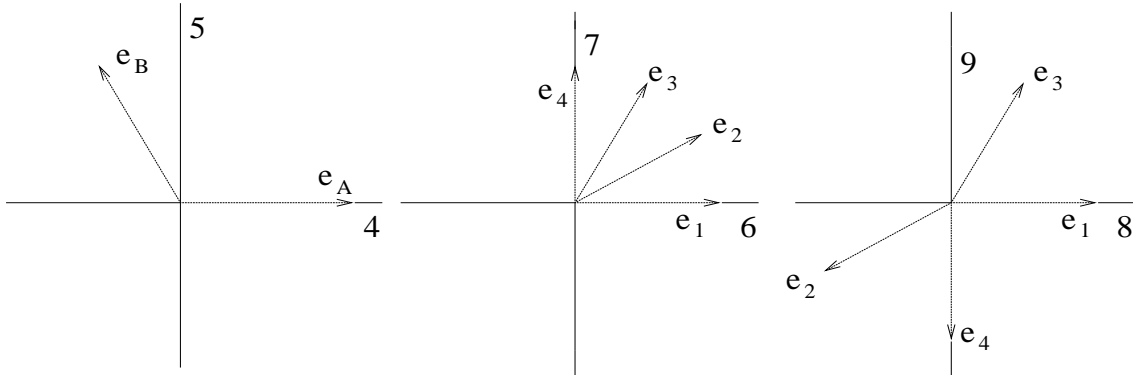


Figure 1: The \mathbb{Z}_{12} lattice vectors. The arrow marked \mathbf{e}_i in each plane is not \mathbf{e}_i itself; rather, it is the component of \mathbf{e}_i in that plane.

per se, but rather in the lattice derived from it. Also, the simple roots in general are of different magnitude, but our construction generates basis vectors having the same size. Thus the basis we use, although a perfectly good basis for the lattice, does not generally consist of root vectors. We will see an example of this in the \mathbb{Z}'_8 case below.

For the factorisable $T^2 \times T^2 \times T^2$ case, it was found that there are two distinct ways of implementing the ΩR projection in each T^2 . These were called **A** and **B** type lattices, and correspond to the R fixed plane being either along the root vectors or at a rotation of $\omega^{\frac{1}{2}}$. One effect of using more generic lattices is to reduce this freedom - the action of R in one rotation plane determines its action in another. For each independent torus - of whatever dimension - in the lattice, there are two possible crystallographic actions of ΩR . As was observed for the factorisable cases in [4] [6], in certain models the tree channel amplitudes had the peculiar feature that the different contributions had the right prefactor to be interpreted as a complete projector. In fact this feature served as a guiding principle for model building and it was even claimed that it is necessary for consistency of the model. This claim was corrected in [47] where it was stated that the other choices of the orientifold action also lead to consistent models. In section 4 we will reconsider this issue for the factorisable case and explicitly construct all the consistent models where the complete projector does not appear.

We will implement the action of ΩR on the closed string modes as

$$\begin{aligned} (\Omega R)\psi_r(\Omega R)^{-1} &= \tilde{\psi}_r \\ (\Omega R)\tilde{\psi}_r(\Omega R)^{-1} &= \psi_r \end{aligned} \tag{5}$$

and likewise for the $\alpha_r, \tilde{\alpha}_r$ oscillators. The loop channel amplitudes contributing

to R-R exchange in tree channel are then

$$\begin{aligned}
KB &= c \int_0^\infty \frac{dt}{t^3} \text{Tr}_{NSNS} \left(\Omega R \frac{(1 + \Theta + \dots + \Theta^{N-1})}{N} e^{-2\pi t(L_0 + \bar{L}_0)} \right) \\
A &= \frac{c}{4} \int_0^\infty \frac{dt}{t^3} \text{Tr}_{NS} \left((-1)^F \frac{(1 + \Theta + \dots + \Theta^{N-1})}{N} e^{-2\pi t L_0} \right) \\
MS &= -\frac{c}{4} \int_0^\infty \frac{dt}{t^3} \text{Tr}_R \left(\Omega R \frac{(1 + \Theta + \dots + \Theta^{N-1})}{N} e^{-2\pi t L_0} \right)
\end{aligned} \tag{6}$$

Here $c \equiv V_4/(8\pi^2\alpha')^2$ arises from the integration over non-compact momenta. These amplitudes involve combinations of ϑ functions and lattice sums. We transform these amplitudes to tree channel using

$$t = \begin{cases} \frac{1}{2l} & \text{Annulus} \\ \frac{1}{4l} & \text{Klein Bottle} \\ \frac{1}{8l} & \text{Möbius Strip} \end{cases} \tag{7}$$

As $R\Theta^k = \Theta^{n-k}R$, $(\Omega R\Theta^k)^2 = 1$ and so we expect only untwisted states to propagate in tree channel. The oscillator contributions in a given twisted sector are straightforward. We convert these to tree channel using the modular transformation properties of the ϑ functions. These, together with the resulting tree channel expressions, are given in the appendix. The lattice contributions are more involved and will be considered below.

In the Klein bottle trace, all insertions in the trace give rise to the same oscillator contribution. However, insertions of the form $\Omega R\Theta^{2k}$ and $\Omega R\Theta^{2k+1}$ generically give rise to different lattice contributions. For the annulus and Möbius sectors, the branes are placed at orientations related by $\Theta^{\frac{1}{2}}$. ‘Twisted sector’ open string amplitudes then correspond to strings stretching between branes at angles. The only non-vanishing insertions in the annulus amplitude are 1 and, if N is even, $\Theta^{\frac{N}{2}}$. The latter insertion leaves all the D6-branes invariant and hence induces an action on the Chan-Paton factors described by a matrix $\gamma_{\frac{N}{2}}$. The twisted tadpole cancellation condition then implies $\text{tr}(\gamma_{\frac{N}{2}}) = 0$. As this is the sole effect of this insertion, when we consider particular models we will not write out explicitly the amplitudes arising from this term.

In the Möbius amplitude, only $(6_i, 6_{i+2\lambda})$ strings can be invariant under an $\Omega R\Theta^k$ insertion and thus contribute in the Möbius strip amplitude. There are two insertions under which such strings are invariant, schematically $\Omega R\Theta^\lambda$ and $\Omega R\Theta^{\lambda+\frac{N}{2}}$. These contribute to the Θ^λ and $\Theta^{\lambda+\frac{N}{2}}$ twisted sectors. For both the annulus and Möbius strip amplitudes, strings starting on the 6_{2k} and 6_{1+2k} branes generically give different lattice contributions.

2.2 Dealing with non-factorisable lattices

For a non-factorisable lattice it is not obvious how the lattice modes should be computed. In sectors where there are fixed tori the lattice contributes momentum and winding modes to the partition function. If general momentum and winding modes can be written

$$\begin{aligned}\mathbf{p} &= \sum n_i \mathbf{p}_i \\ \mathbf{w} &= \sum m_i \mathbf{w}_i, \quad m_i, n_i \in \mathbb{Z}\end{aligned}\tag{8}$$

then the loop channel partition function contains a sum

$$\sum_{n_i} \exp(-\delta \pi t n_i M_{ij} n_j) \sum_{m_i} \exp(-\delta \pi t m_i W_{ij} m_j)\tag{9}$$

where $n_i, m_i \in \mathbb{Z}$, $M_{ij} = \mathbf{p}_i \cdot \mathbf{p}_j$, $W_{ij} = \mathbf{w}_i \cdot \mathbf{w}_j$ and $\delta = \begin{cases} 1 & \text{Klein bottle} \\ 2 & \text{Annulus, Möbius strip} \end{cases}$

We then transform to tree channel using

$$t = \begin{cases} \frac{1}{2l} & \text{Annulus} \\ \frac{1}{4l} & \text{Klein Bottle} \\ \frac{1}{8l} & \text{Möbius Strip} \end{cases}\tag{10}$$

and the generalised Poisson resummation formula

$$\sum_{n_i} \exp(-\pi t n_i A_{ij} n_j) = \frac{1}{t^{\frac{\dim(A)}{2}} (\det A)^{\frac{1}{2}}} \sum_{n_i} \exp(-\frac{\pi}{t} n_i A_{ij}^{-1} n_j).\tag{11}$$

To find the momentum modes we need to find vectors in the dual lattice invariant under ΩR . The appropriate dual lattice differs in open and closed sectors. Closed strings can move freely throughout the lattice and so the dual lattice is that of the T^6 . Open strings are tied to a brane and the dual lattice is that of the vectors spanning the brane. Winding modes are perpendicular to the momentum modes. In the annulus case, all winding modes running from a brane to itself contribute to the sum (9). In the Klein bottle and Möbius strip amplitudes, there is an insertion of ΩR into the trace. In the Möbius strip amplitudes, where there are generically open string winding modes that are fractional multiples of lattice vectors, the insertion of ΩR in the trace can cause the centre of mass coordinate of the string to be shifted by

$$T : \mathbf{x} \rightarrow \mathbf{x} + \mathbf{a}.\tag{12}$$

T acts on momentum modes as

$$T|\mathbf{p}\rangle = \exp(2\pi i \mathbf{p} \cdot \mathbf{a})|\mathbf{p}\rangle.\tag{13}$$

In the particular case where $\mathbf{p} = \frac{n\mathbf{e}_x}{R}$ and $\mathbf{T} : \mathbf{x} \rightarrow \mathbf{x} + \frac{R}{2}\mathbf{e}_x$, the sum over momentum modes in (9) is then

$$\sum_{n_i} (-1)^{n_i} \exp(-\pi t n_i A_{ij} n_j). \quad (14)$$

Transformed to tree channel, this sum does not actually diverge in the $l \rightarrow \infty$ limit and so such winding modes do not contribute to the tadpoles. Lattice modes also occur when one complex plane is left invariant under the orbifold action, when an analogous version of the above discussion applies.

The lattice also contributes to the amplitude through fixed points and brane intersection numbers. For a non-factorisable lattice, it is difficult to find these visually. For the former, the Lefschetz fixed point theorem is not sufficient as we also need to know which points are invariant under the action of ΩR . We therefore need to compute explicitly the location of the fixed points using the action of ω . This is tedious but not difficult. A useful reference for this and other details of the non-factorisable lattices is [48], although the lattice bases used there differ from ours. To calculate brane intersection numbers we need to find a spanning set of lattice vectors for each of the branes. The intersection points are then given by solving a set of equations of the schematic form

$$\sum \alpha_i \mathbf{v}_i = \sum \beta_i \mathbf{w}_i \quad (15)$$

for nontrivial (not in \mathbb{Z}) values of α_i . In the case of the Möbius strip, we also need to investigate whether the intersection points are invariant under $\Omega R \Theta^k$ for the appropriate value of k .

Actually, for the annulus amplitude we would like to present a simple method for calculating the contribution of the lattice modes and the intersection numbers. Let \mathbf{e}_i be the basis vectors of the lattice and let $g_{ij} = \mathbf{e}_i \cdot \mathbf{e}_j$. Let $\mathbf{v}_i, i = 1, 2, 3$ be the lattice vectors that describe the 3-cycle wrapped by the brane, such that any point \mathbf{x} on the brane can be uniquely written

$$\mathbf{x} = \sum \alpha_i \mathbf{v}_i \quad \alpha_i \in [0, 1). \quad (16)$$

We then define $(M_A)_{ij} = \mathbf{v}_i \cdot \mathbf{v}_j$. The lattice dual to the brane is now given by $\mathbf{v}_i^* = \mathbf{v}_j (M_A^{-1})_{ji}$, with $\mathbf{v}_i^* \cdot \mathbf{v}_j^* = (M_A^{-1})_{ij}$. The contribution of momentum modes to the one-loop amplitude is then

$$\sum_{n_i} \exp(-2\pi t n_i (M_A^{-1})_{ij} n_j) \rightarrow l^{\frac{\dim(M_A)}{2}} (\det M_A)^{\frac{1}{2}} \sum_{n_i} \exp(-\pi l n_i (M_A)_{ij} n_j). \quad (17)$$

Suppose a generic winding mode is written

$$\mathbf{w} = \sum m_i \mathbf{w}_i \quad m_i \in \mathbb{Z}, \quad (18)$$

then any vector \mathbf{v} in the fundamental cell can be uniquely written as

$$\mathbf{v} = \sum (\alpha_i \mathbf{v}_i + \beta_i \mathbf{w}_i) \quad \alpha, \beta \in [0, 1). \quad (19)$$

As \mathbf{v}_i and \mathbf{w}_i are linearly independent, every point is expressible as a linear combination of the two sets of vectors. Because \mathbf{v}_i are lattice vectors, and \mathbf{w}_i returns to the brane, all cases with α or $\beta > 1$ are reducible to the range given. Finally, if there were two distinct expressions for \mathbf{v} , then by taking the difference we would find a winding mode not expressible in the form of (18), in contradiction of the original assumption.

We now define $(W_A)_{ij} = \mathbf{w}_i \cdot \mathbf{w}_j$. The winding contribution to the partition function is

$$\sum_{m_i} \exp(-2\pi t m_i (W_A)_{ij} m_j) \rightarrow \frac{l^{\frac{\dim(W_A)}{2}}}{(\det W_A)^{\frac{1}{2}}} \sum_{m_i} \exp(-\pi l m_i (W_A^{-1})_{ij} m_j). \quad (20)$$

Now, for any set of vectors \mathbf{u}_i , $(\det(\mathbf{u}_i \cdot \mathbf{u}_j))^{\frac{1}{2}}$ gives the volume spanned by that set of vectors. Together, \mathbf{v}_i and \mathbf{w}_i span the fundamental cell. As

$$(\text{Vol. of fund. cell}) = (\text{Vol. along brane}) \times (\text{Vol. transverse to brane})$$

we can conclude that

$$(\det W_A)^{\frac{1}{2}} = \frac{(\det g)^{\frac{1}{2}}}{(\det M_A)^{\frac{1}{2}}}. \quad (21)$$

Combining (17) and (20), we see that in the $l \rightarrow \infty$ limit the tree channel lattice factor is simply

$$\frac{(\det M_A)}{(\det g)^{\frac{1}{2}}} \quad (22)$$

which has a nice geometric interpretation and also determines the normalisation of the boundary state for branes wrapping toroidal cycles, as that is found by comparison with the 1-loop annulus amplitude.

There is likewise a nice formula for the intersection number of two branes wrapping distinct 3-cycles. Suppose we have two branes, spanned by vectors $\mathbf{v}_i, \mathbf{v}'_i$ such that for each brane (16) is satisfied. We can write each vector in components $\mathbf{v}_i = \sum v_{ij} \mathbf{e}_j$. We then define

$$I = \det \begin{pmatrix} v_{11} & v_{12} & \dots & v_{16} \\ v_{21} & v_{22} & \dots & v_{26} \\ \dots & \dots & \dots & \dots \\ v'_{31} & v'_{32} & \dots & v'_{36} \end{pmatrix}. \quad (23)$$

I measures the number of fundamental cells spanned by the combination of the two branes. Now, if the two branes span I fundamental cells, then it means that they span I points equivalent to the origin. That is, we have I solutions to

$$\sum \alpha_i \mathbf{v}_i + \sum \beta_i \mathbf{v}'_i \equiv 0 \quad \alpha_i, \beta_i \in [0, 1). \quad (24)$$

However, (24) is equivalent to the existence of I sets of (α_i, β_i) such that

$$\sum \alpha_i \mathbf{v}_i \equiv - \sum \beta_i \mathbf{v}'_i \quad \alpha_i, \beta_i \in [0, 1), \quad (25)$$

and therefore I is nothing else than the intersection number of the two branes. Formula (23) generalises the familiar case of a 2-torus, where branes with wrapping numbers (m_1, n_1) , (m_2, n_2) have intersection number $m_1 n_2 - n_1 m_2$.

The above formulae are simple and require no detailed calculation. In the case of the Möbius strip and Klein bottle amplitudes, it would be nice to have an equally elegant way of computing the lattice contributions and intersection numbers, given the action of ΩR on the lattice. Even though R will just act as a projection on the modes, such a formula has eluded us. We must therefore explicitly compute modes and intersection points invariant under ΩR .

Suppose we have found generators of momentum modes \mathbf{p}_i (Klein bottle) or vectors \mathbf{v}_i spanning the brane (annulus or Möbius strip), and also winding modes \mathbf{w}_i in the lattice. Then we define

$$\begin{aligned} (M_{KB})_{ij} &= \mathbf{p}_i \cdot \mathbf{p}_j \\ (M_{MS})_{ij} = (M_A)_{ij} &= \mathbf{v}_i \cdot \mathbf{v}_j \\ (W_{KB})_{ij} = (W_{MS})_{ij} &= \mathbf{w}_i \cdot \mathbf{w}_j. \end{aligned} \quad (26)$$

Then, if $\dim(M) = \dim(W) = n$, the tree channel lattice mode contributions are

$$KB : \frac{4^n}{(\det M_{KB} \det W_{KB})^{\frac{1}{2}}} \quad A : \frac{(\det M_A)^{\frac{1}{2}}}{(\det g)^{\frac{1}{2}}} \quad MS : \frac{4^n (\det M_{MS})^{\frac{1}{2}}}{(\det W_{MS})^{\frac{1}{2}}}. \quad (27)$$

Once we have computed the lattice modes, twisted sector fixed points, and brane intersection numbers, we can write down the tree-channel amplitudes as prescribed in the appendix.

3 The massless spectrum

3.1 The closed string spectrum

The computation of the closed string spectrum follows the pattern outlined in [6]. Closed string states in the Θ^k twisted sector live at Θ^k fixed points and must be invariant under both the orbifold and orientifold projection. It is simplest first to work out the orbifold states and then to analyse their behaviour under the action of ΩR . In general, the fixed points of a Θ^k twisted sector decompose into orbits of maximal length k under the action of Θ . If a fixed point is in an orbit of length N , then under Θ the oscillator part of a state $|L\rangle \otimes |R\rangle$ can have a phase of $e^{\frac{2\pi i}{N}}$ or any multiple thereof.

Once we have the orbifold states, we keep only those invariant under ΩR . For an orbit taken onto itself, we keep the symmetric part of the NS-NS sector

and the antisymmetric part of the R-R sector. For orbits exchanged among themselves, symmetrisation and anti-symmetrisation results in a single full copy of both sectors being retained. The net result is some number of chiral and vector multiplets in each twisted sector. The total number of such multiplets in each sector is given by the contribution of that sector to $h^{1,1} + h^{2,1}$ (cf [49]).

3.2 The open string spectrum

In orientifold models the open string sector is determined by tadpole cancellation. This determines whether the action of ΩR and $\Theta^{\frac{N}{2}}$ on the Chan-Paton indices is the symplectic or orthogonal projection. Once $\gamma_{\Omega R}$ and $\gamma_{\frac{N}{2}}$ are known, to find the spectrum we simply look for states invariant under their action [50].

The projection is determined by the relative sign of the Möbius strip amplitude. In the Klein bottle amplitude (6), the \pm sign in front of each twisted sector is determined by the action of ΩR on the ground state.

$$\Omega R|0\rangle \otimes |0\rangle_{NSNS} = \pm |0\rangle \otimes |0\rangle_{NSNS} \quad (28)$$

This in turn is fixed by the requirement that $\Omega R|p_1\rangle \otimes |p_2\rangle_{NSNS} = |p_1\rangle \otimes |p_2\rangle_{NSNS}$, where $|p_1\rangle$ and $|p_2\rangle$ are physical NS states and thus bosonic. Using our conventions (5), $(\Omega R)\psi_r\psi_r(\Omega R)^{-1} = -\psi_r\psi_r$. Thus, if the ground state is physical we obtain a leading $+$ sign and if the ground state is unphysical we obtain a leading $-$ sign. The leading sign in the annulus amplitude is given by $(-1)^F|0\rangle$. As $(-1)^F$ determines whether or not a state is physical through the GSO projection, the result is that in any twisted sector the annulus and Klein bottle always have the same sign.

The Möbius strip signs are more delicate. For odd orbifolds (i.e. the \mathbb{Z}_3 and the \mathbb{Z}_7) the only non-trivial action on the Chan-Paton indices is that of ΩR . Strings stretching between the 6_i and $6_{(i+2k)}$ branes contribute to the Θ^k twisted sector under an appropriate insertion of $\Omega R\Theta^\lambda$. For even orbifolds, $(i, i+2k)$ strings contribute to the Θ^k and $\Theta^{k+\frac{N}{2}}$ sectors.

The leading sign in the Möbius amplitude, for an insertion of $\Omega R\Theta^\lambda$, is given by the action of $\Omega R\Theta^\lambda$ on the ground state. This sign has several contributions. First, $\Omega R|0\rangle_R = -|0\rangle_R$, e.g. see [51]. Θ^λ may also have some action on the ground state. Finally, twisted open strings are located at brane intersection points, which may be interchanged under the action of $\Omega R\Theta^\lambda$. Symmetrising and anti-symmetrising these may also give extra signs. Once all the signs are fixed, we can then use tadpole cancellation to determine $\gamma_{\Omega R}$ and $\gamma_{\frac{N}{2}}$.

There are several issues arising in the computation of the open string sector. First, in the above procedure we obtain sector-by-sector tadpole cancellation. This is more stringent than necessary; the vanishing of R-R flux just requires that the overall tadpole cancel. Secondly, there are cases where tadpole cancellation does not seem to determine the form of $\gamma_{\Omega R}$ or $\gamma_{\frac{N}{2}}$. These arise when the partition

function in a twisted sector contains a $\vartheta \left[\begin{smallmatrix} \frac{1}{2} \\ \frac{1}{2} \end{smallmatrix} \right]$ part, which vanishes. Indeed, for \mathbb{Z}_4 orbifolds all twisted sector partition functions vanish.

We take the view that these vanishing sectors in a certain sense vanish accidentally. To determine the open string spectrum, we require that we still obtain tadpole cancellation under a small formal deformation of the twist, e.g. $(\frac{1}{4}, \frac{1}{4}, \frac{1}{2}) \rightarrow (\frac{1}{4}, \frac{1}{4} + \epsilon, \frac{1}{2} + \epsilon)$. This procedure allows a determination of the spectrum and, applied to the cases studied in [4][6], results in the same spectrum as found there.

4 Examples of factorisable orientifolds revisited

As previously explained, we can relax the requirement that the complete projector appear in all three (Klein bottle, annulus and Möbius strip) amplitudes, yielding models which generically have different gauge groups carried by 6_{2i} and 6_{2i+1} branes. In some cases the gauge groups are the same, but the massless open string spectrum is not invariant under the exchange of the two gauge group factors, similarly to the \mathbb{Z}'_6 case in [6]. We found that all the various ΩR implementations for the $\mathbb{Z}_4, \mathbb{Z}_6, \mathbb{Z}'_6$ models yield consistent solutions⁴. Their closed and open string spectra are shown in tables 3,4 and 5. We use $\mathbf{1}_0$ to denote a $U(2)$ singlet uncharged under the gauge group.

Table 3: Closed string spectra

Model	Θ^0	$\Theta + \Theta^{-1}$	$\Theta^2(+\Theta^{-2})$	Θ^3
\mathbb{Z}_4 (AAA)	6C	16C	16C	absent
\mathbb{Z}_4 (AAB)	6C	12C+4V	16C	absent
\mathbb{Z}_6 (AAA)	5C	2C+1V	10C+5V	10C+1V
\mathbb{Z}_6 (BBB)	5C	3C	15C	10C+1V
\mathbb{Z}'_6 (AAA)	4C	7C+5V	14C+4V	10C+2V
\mathbb{Z}'_6 (BBB)	4C	9C+3V	18C	10C+2V

Since for the factorisable \mathbb{Z}_4 models with $v = \frac{1}{4}(1, 1, -2)$, $\Omega R\Theta$ takes an **A**-type lattice into a **B**-type lattice in the first two tori, and thus the **AAA** and **BBA**, **AAB** and **BBB** to be equivalent to each other. Similarly, models **AAA** and **BBA**, **AAB** and **BBB** for \mathbb{Z}_6 as well as **AAA** and **BAB**, **ABA** and **BBB** for \mathbb{Z}'_6 are equivalent.

⁴One can also revisit the 6-dimensional orientifolds of [4]. We again find consistent models, and the computed spectrum is anomaly free.

Table 4: The \mathbb{Z}_4 open string spectra

Model	$(6_i, 6_i)$	$(6_i, 6_{i+1})$	$(6_i, 6_{i+2})$
AAA	$U(16) \times U(4)$ (1V+1C) $(\mathbf{256}, \mathbf{1}) \oplus (\mathbf{1}, \mathbf{16}) +$ 2C $(\mathbf{120}, \mathbf{1}) \oplus (\overline{\mathbf{120}}, \mathbf{1}) +$ 2C $(\mathbf{1}, \mathbf{6}) \oplus (\mathbf{1}, \overline{\mathbf{6}})$	1C $(\mathbf{16}, \mathbf{4}) \oplus (\overline{\mathbf{16}}, \mathbf{4})$	2C $(\mathbf{256}, \mathbf{1}) + 8\text{C } (\mathbf{1}, \mathbf{16})$
AAB	$U(8) \times U(2)$ (1V+1C) $(\mathbf{64}, \mathbf{1}_0) \oplus (\mathbf{1}, \mathbf{4}) +$ 2C $(\mathbf{28}, \mathbf{1}_0) \oplus (\overline{\mathbf{28}}, \mathbf{1}_0) +$ 2C $(\mathbf{1}, \mathbf{1}) \oplus (\mathbf{1}, \overline{\mathbf{1}})$	2C $(\mathbf{8}, \mathbf{2}) \oplus (\overline{\mathbf{8}}, \mathbf{2})$	2C $(\mathbf{64}, \mathbf{1}_0) + 8\text{C } (\mathbf{1}, \mathbf{4})$

5 Examples of non-factorisable orientifolds

In this section we discuss in some detail a couple of completely new examples of ΩR orientifolds on non-factorisable orbifolds. Employing the general formalism developed in section 2 and section 3 we consider the solutions to the tadpole cancellation conditions where we place the D6-branes parallel to the orientifold planes. The closed string spectrum for all models considered in this section is computed as in section 3 and appears in table 6.

5.1 \mathbb{Z}_7 Model : A_7 with $v = \frac{1}{7}(1, 2, -3)$

The $SU(7)$ algebra has six root vectors, denoted by \mathbf{e}_i . They are of equal magnitude (taken to be 1), and $g_{ij} = \mathbf{e}_i \cdot \mathbf{e}_j$ is given by

$$g_{ij} = \begin{pmatrix} 1 & -\frac{1}{2} & 0 & 0 & 0 & 0 \\ -\frac{1}{2} & 1 & -\frac{1}{2} & 0 & 0 & 0 \\ 0 & -\frac{1}{2} & 1 & -\frac{1}{2} & 0 & 0 \\ 0 & 0 & -\frac{1}{2} & 1 & -\frac{1}{2} & 0 \\ 0 & 0 & 0 & -\frac{1}{2} & 1 & -\frac{1}{2} \\ 0 & 0 & 0 & 0 & -\frac{1}{2} & 1 \end{pmatrix} \quad (29)$$

The Weyl element Γ_i reflects across the plane perpendicular to a root vector. Its action on a vector \mathbf{x} is given by

$$\Gamma_i \mathbf{x} = \mathbf{x} - 2 \frac{\mathbf{e}_i \cdot \mathbf{x}}{\mathbf{e}_i \cdot \mathbf{e}_i} \mathbf{e}_i \quad (30)$$

The Coxeter element $\omega = \Gamma_1 \Gamma_2 \dots \Gamma_6$ acts as

$$\begin{aligned} \omega \mathbf{e}_i &= \mathbf{e}_{i+1} & i = 1, 2, 3, 4, 5 \\ \omega \mathbf{e}_6 &= -\mathbf{e}_1 - \mathbf{e}_2 - \mathbf{e}_3 - \mathbf{e}_4 - \mathbf{e}_5 - \mathbf{e}_6 \end{aligned} \quad (31)$$

Table 5: $\mathbb{Z}_6, \mathbb{Z}'_6$ open spectra

Model	$(6_i, 6_i)$	$(6_i, 6_{i+1})$	$(6_i, 6_{i+2})$	$(6_i, 6_{i+3})$
\mathbb{Z}_6 AAA	$U(2) \times U(2)$ (1C+1V) $(\mathbf{4}, \mathbf{1}_0) \oplus (\mathbf{1}_0, \mathbf{4}) +$ $2C (\mathbf{1}, \mathbf{1}_0) \oplus (\bar{\mathbf{1}}, \mathbf{1}_0) +$ $2C (\mathbf{1}_0, \mathbf{1}) \oplus (\mathbf{1}_0, \bar{\mathbf{1}})$	$1C (\mathbf{2}, \mathbf{2}) \oplus$ $(\bar{\mathbf{2}}, \mathbf{2})$	$8C (\mathbf{3}, \mathbf{1}_0) \oplus (\bar{\mathbf{3}}, \mathbf{1}_0) +$ $5C (\mathbf{4}, \mathbf{1}_0) + 1C (\mathbf{1}_0, \bar{\mathbf{4}})$	$4C (\mathbf{2}, \mathbf{2}) \oplus$ $(\bar{\mathbf{2}}, \mathbf{2})$
\mathbb{Z}_6 BBB	$U(2) \times U(2)$ (1C+1V) $(\mathbf{4}, \mathbf{1}_0) \oplus (\mathbf{1}_0, \mathbf{4}) +$ $2C (\mathbf{1}, \mathbf{1}_0) \oplus (\bar{\mathbf{1}}, \mathbf{1}_0) +$ $2C (\mathbf{1}_0, \mathbf{1}) \oplus (\mathbf{1}_0, \bar{\mathbf{1}})$	$3C (\mathbf{2}, \mathbf{2}) \oplus$ $(\bar{\mathbf{2}}, \mathbf{2})$	$24C (\mathbf{3}, \mathbf{1}_0) \oplus (\bar{\mathbf{3}}, \mathbf{1}_0) +$ $15C (\mathbf{4}, \mathbf{1}_0) + 3C (\mathbf{1}_0, \bar{\mathbf{4}})$	$4C (\mathbf{2}, \mathbf{2}) \oplus$ $(\bar{\mathbf{2}}, \mathbf{2})$
\mathbb{Z}'_6 AAA	$U(2) \times U(2)$ (1C+1V) $(\mathbf{4}, \mathbf{1}_0) \oplus (\mathbf{1}_0, \mathbf{4}) +$ $2C (\mathbf{1}, \mathbf{1}_0) \oplus (\bar{\mathbf{1}}, \mathbf{1}_0) +$ $2C (\mathbf{1}_0, \mathbf{1}) \oplus (\mathbf{1}_0, \bar{\mathbf{1}})$	$2C (\mathbf{2}, \mathbf{2}) \oplus$ $(\bar{\mathbf{2}}, \mathbf{2})$	$1C (\mathbf{1}, \mathbf{1}_0) \oplus (\bar{\mathbf{1}}, \mathbf{1}_0) +$ $3C (\mathbf{1}_0, \mathbf{1}) \oplus (\mathbf{1}_0, \bar{\mathbf{1}}) +$ $1C (\mathbf{4}, \mathbf{1}_0) + 3C (\mathbf{1}_0, \mathbf{4})$	$4C (\mathbf{2}, \mathbf{2}) \oplus$ $(\bar{\mathbf{2}}, \mathbf{2})$
\mathbb{Z}'_6 BBB	$U(2) \times U(2)$ (1C+1V) $(\mathbf{4}, \mathbf{1}_0) \oplus (\mathbf{1}_0, \mathbf{4}) +$ $2C (\mathbf{1}, \mathbf{1}_0) \oplus (\bar{\mathbf{1}}, \mathbf{1}_0) +$ $2C (\mathbf{1}_0, \mathbf{1}) \oplus (\mathbf{1}_0, \bar{\mathbf{1}})$	$6C (\mathbf{2}, \mathbf{2}) \oplus$ $(\bar{\mathbf{2}}, \mathbf{2})$	$9C (\mathbf{1}, \mathbf{1}_0) \oplus (\bar{\mathbf{1}}, \mathbf{1}_0) +$ $3C (\mathbf{1}_0, \mathbf{1}) \oplus (\mathbf{1}_0, \bar{\mathbf{1}}) +$ $9C (\mathbf{4}, \mathbf{1}_0) + 3C (\mathbf{1}_0, \mathbf{4})$	$4C (\mathbf{2}, \mathbf{2}) \oplus$ $(\bar{\mathbf{2}}, \mathbf{2})$

ω manifestly satisfies $\omega^7 = 1$. As discussed in section 2.1, the action of ω can be written as

$$\begin{aligned} Z_i &\rightarrow \exp(2\pi i v_i) Z_i \\ \bar{Z}_i &\rightarrow \exp(-2\pi i v_i) \bar{Z}_i, \end{aligned} \quad (32)$$

where $v_i = (\frac{1}{7}, \frac{2}{7}, -\frac{3}{7})$ and the Z_i are coordinates in some orthogonal complex planes. The lattice vectors are visualised as in figure 2.

By inspection, ΩR acts crystallographically as

$$\begin{aligned} \mathbf{e}_1 &\rightarrow \mathbf{e}_1 \\ \mathbf{e}_2 &\rightarrow -\mathbf{e}_1 - \mathbf{e}_2 - \mathbf{e}_3 - \mathbf{e}_4 - \mathbf{e}_5 - \mathbf{e}_6 \\ \mathbf{e}_3 &\rightarrow \mathbf{e}_6 \\ \mathbf{e}_4 &\rightarrow \mathbf{e}_5 \\ \mathbf{e}_5 &\rightarrow \mathbf{e}_4 \\ \mathbf{e}_6 &\rightarrow \mathbf{e}_3. \end{aligned} \quad (33)$$

In the Klein bottle amplitude, lattice modes only contribute in the untwisted sector. The momentum modes are in the dual lattice and have the general form

$$\alpha(2\mathbf{e}_1) + \beta(2\mathbf{e}_3 + 2\mathbf{e}_6) + \gamma(2\mathbf{e}_4 + 2\mathbf{e}_5), \quad (34)$$

Table 6: Closed string spectra

Model	Θ^0	$\Theta + \Theta^{-1}$	$\Theta^2 + \Theta^{-2}$	$\Theta^3 + \Theta^{-3}$	$\Theta^4 (+\Theta^{-4})$	$\Theta^5 + \Theta^{-5}$	Θ^6
$\mathbb{Z}_7(\mathbf{A})$	3C	4C+3V	4C+3V	4C+3V	absent	absent	absent
$\mathbb{Z}_7(\mathbf{B})$	3C	7C	7C	7C	absent	absent	absent
$\mathbb{Z}_8(\mathbf{AA})$	4C	8C	8C	8C	10C	absent	absent
$\mathbb{Z}_8(\mathbf{BA})$	4C	6C+2V	8C	6C+2V	10C	absent	absent
$\mathbb{Z}'_8(\mathbf{AA})$	3C	4C	10C	4C	9C	absent	absent
$\mathbb{Z}'_8(\mathbf{BA})$	3C	4C	9C + 1V	4C	9C	absent	absent
$\mathbb{Z}_{12}(\mathbf{AA})$	3C	2C+1V	2C+1V	6C	6C + 3V	2C + 1V	7C
$\mathbb{Z}_{12}(\mathbf{BA})$	3C	3C	3C	6C	9C	3C	7C
$\mathbb{Z}'_{12}(\mathbf{AA})$	4C	4C	2C	8C	10C	4C	6C
$\mathbb{Z}'_{12}(\mathbf{BA})$	4C	3C+1V	2C	6C + 2V	10C	3C + 1V	6C

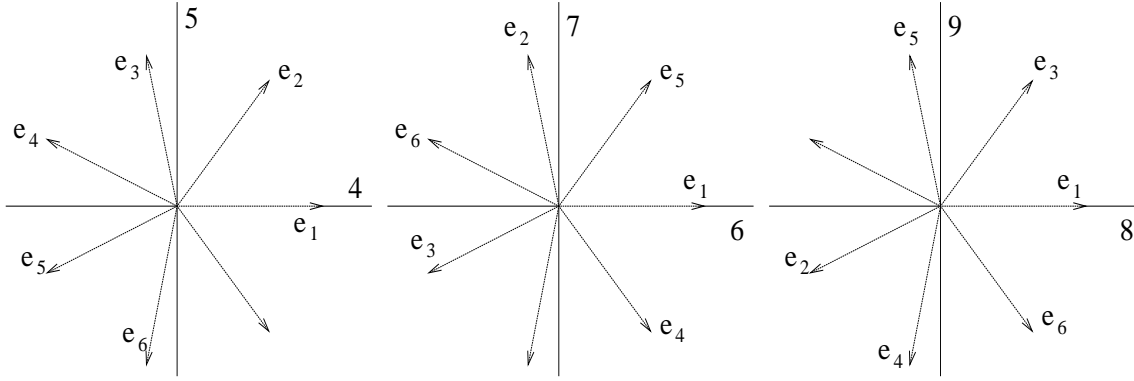


Figure 2: The \mathbb{Z}_7 lattice

where $\alpha, \beta, \gamma \in \mathbb{Z}$. The winding modes are

$$\alpha'(\mathbf{e}_1 + 2\mathbf{e}_2 + \mathbf{e}_3 + \mathbf{e}_4 + \mathbf{e}_5 + \mathbf{e}_6) + \beta'(\mathbf{e}_3 - \mathbf{e}_6) + \gamma'(\mathbf{e}_4 - \mathbf{e}_5) \quad (35)$$

with $\alpha', \beta', \gamma' \in \mathbb{Z}$. We then get

$$M_{KB} = 4 \begin{pmatrix} 1 & 0 & 0 \\ 0 & 2 & -1 \\ 0 & -1 & 1 \end{pmatrix} \quad (36)$$

$$W_{KB} = \begin{pmatrix} 2 & -1 & 0 \\ -1 & 2 & -1 \\ 0 & -1 & 3 \end{pmatrix}. \quad (37)$$

The untwisted lattice factor is then $\frac{64}{(\det M_{KB})^{\frac{1}{2}}(\det W_{KB})^{\frac{1}{2}}} = \frac{8}{\sqrt{7}}$. The $SU(7)$ lattice

has 7 fixed points in each twisted sector. These are $\frac{n}{7}(\mathbf{e}_1 + 2\mathbf{e}_2 + 3\mathbf{e}_3 + 4\mathbf{e}_4 + 5\mathbf{e}_5 + 6\mathbf{e}_6)$, where $n = 0, 1, \dots, 6$. It is easily verified that only the $n = 0$ case is invariant under ΩR .

We can now write down the tree channel Klein bottle amplitude. As the zero point energy in all sectors is negative, $\Omega R|0\rangle \otimes |0\rangle = -|0\rangle \otimes |0\rangle$, and all sectors carry a leading minus sign

$$\begin{aligned} KB &= c \int_0^\infty 16l dl \left(\frac{-1}{16l^4}(\Theta^0) \frac{8l^3}{\sqrt{7}} - \frac{1}{2l}(\Theta) - \dots - \frac{1}{2l}(\Theta^6) \right) \\ &= c \int_0^\infty dl \frac{8}{\sqrt{7}} \left(-(\Theta^0) - \sqrt{7}(\Theta^1) - \sqrt{7}(\Theta^2) - \dots - \sqrt{7}(\Theta^6) \right). \end{aligned} \quad (38)$$

As $\sin(\frac{\pi}{7}) \sin(\frac{2\pi}{7}) \sin(\frac{4\pi}{7}) = \frac{\sqrt{7}}{8}$, we actually have the complete projector $\prod_i 2 \sin(\pi v_i)$ appearing here.

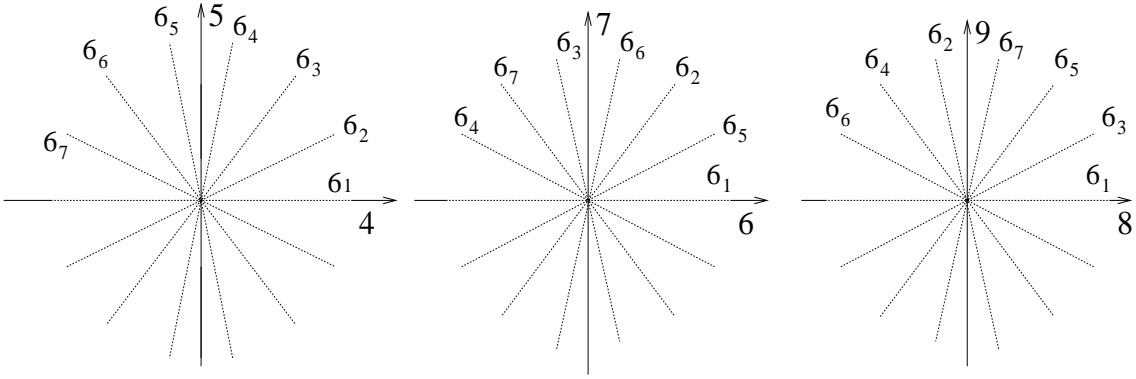


Figure 3: The \mathbb{Z}_7 branes

In the limit $l \rightarrow \infty$, the amplitude (38) diverges. We add D-branes as shown in figure 3. The volume occupied by the 1 brane is

$$\alpha' \mathbf{e}_1 + \beta'(\mathbf{e}_3 + \mathbf{e}_6) + \gamma'(\mathbf{e}_4 + \mathbf{e}_5) \quad (39)$$

with $\alpha', \beta', \gamma' \in [0, 1)$ and therefore

$$M_A = \begin{pmatrix} 1 & 0 & 0 \\ 0 & 2 & -1 \\ 0 & -1 & 1 \end{pmatrix}. \quad (40)$$

As explained in section 2.2, the lattice mode contribution for the annulus is $\frac{(\det M_A)}{(\det g)^{\frac{1}{2}}} = \frac{8}{\sqrt{7}}$. There are actually no non-trivial brane intersections in the twisted sectors, and so the annulus amplitude is

$$A = M^2 c \int l dl \left(\frac{-1}{16l^4}(\Theta^0) \frac{8l^3}{\sqrt{7}} - \frac{1}{2l}(\Theta) - \dots - \frac{1}{2l}(\Theta^6) \right) \quad (41)$$

which can be simplified to

$$A = M^2 c \int \frac{dl}{2\sqrt{7}} \left(-(\Theta^0) - \sqrt{7}(\Theta) - \dots \sqrt{7}(\Theta^6) \right) \quad (42)$$

As with the Klein bottle amplitude (38), in all sectors the ground state is unphysical and so $(-1)^F|0\rangle = -|0\rangle$.

Finally we need to consider the Möbius strip amplitude. The twisted sector intersection numbers remain trivial. The lattice modes must be invariant under ΩR . As described in section 2.2, we have

$$M_{MS} = M_A = \begin{pmatrix} 1 & 0 & 0 \\ 0 & 2 & -1 \\ 0 & -1 & 1 \end{pmatrix} \quad (43)$$

$$W_{MS} = W_{KB} = \begin{pmatrix} 2 & -1 & 0 \\ -1 & 2 & -1 \\ 0 & -1 & 3 \end{pmatrix} \quad (44)$$

with a resulting lattice factor for the Möbius strip amplitude of $64 \frac{(\det M_{MS})^{\frac{1}{2}}}{(\det W_{MS})^{\frac{1}{2}}} = \frac{64}{\sqrt{7}}$. The Möbius amplitude reads

$$MS = +Mc \int 16dl \left(\frac{1}{2^8 l^4} (\Theta^0) \frac{64l^3}{\sqrt{7}} + \frac{1}{4l} (\Theta) + \dots + \frac{1}{4l} (\Theta^6) \right) \quad (45)$$

giving

$$MS = +Mc \int dl \frac{4}{\sqrt{7}} \left((\Theta^0) + \sqrt{7}(\Theta) + \dots \sqrt{7}(\Theta^6) \right). \quad (46)$$

We have in equation (46) fixed $\text{tr}(\gamma_{\Omega R \Theta^k}^T \gamma_{\Omega R \Theta^k}^{-1}) = +M$ in all sectors. Extracting the leading divergences from equations (38), (42) and (46), the tadpole cancellation conditions are

$$(M^2 - 8M + 16) = 0, \quad (47)$$

implying $M = 4$ and the branes carrying an $SO(4)$ gauge group.

The closed string spectrum was given in table 6. For the open strings, the ΩR projection is the $SO(n)$ projection in all sectors. In each twisted sector, there is one massless oscillator state located at the origin. This being an odd orbifold, there is no additional $\Theta^{\frac{N}{2}}$ projection to concern us and the open string spectrum is as in table 7.

The above action of R is not the only crystallographic implementation. We could also implement R at a rotation of $\Theta^{\frac{1}{2}}$ in the \mathbf{B} orientation. If we repeat the above analysis, we find that all amplitudes are multiplied by 7. This does not affect the tadpole cancellation condition and we again get an $SO(4)$ gauge group. This behaviour is exactly analogous to that encountered for the \mathbb{Z}_3 orientifold in [6].

Table 7: The \mathbb{Z}_7 open string spectrum

Sector	$\mathbb{Z}_7(\mathbf{A})$	$\mathbb{Z}_7(\mathbf{B})$
$(6_i, 6_i)$	$1V(\mathbf{6}) + 3C(\mathbf{6})$	$1V(\mathbf{6}) + 3C(\mathbf{6})$
$(6_i, 6_{i\pm 1})$	$1C(\mathbf{6})$	$7C(\mathbf{6})$
$(6_i, 6_{i\pm 2})$	$1C(\mathbf{6})$	$7C(\mathbf{6})$
$(6_i, 6_{i\pm 3})$	$1C(\mathbf{6})$	$7C(\mathbf{6})$

5.2 \mathbb{Z}'_8 Model: $B_2 \times B_4$ with $v = \frac{1}{8}(2, 1, -3)$

The \mathbb{Z}'_8 case has several subtleties typical of even orientifolds. For \mathbb{Z}'_8 , Θ has $v = \frac{1}{8}(2, 1, -3)$ and is given by the Coxeter element of $B_2 \times B_4$. Using \mathbf{b}_i to denote the simple roots of B_4 ,

$$b_{ij} = \mathbf{b}_i \cdot \mathbf{b}_j = \begin{pmatrix} 2 & -1 & 0 & 0 \\ -1 & 2 & -1 & 0 \\ 0 & -1 & 2 & -2 \\ 0 & 0 & -2 & 4 \end{pmatrix}. \quad (48)$$

We can verify that

$$\begin{aligned} \omega \mathbf{b}_1 &= \mathbf{b}_2 \\ \omega \mathbf{b}_2 &= \mathbf{b}_3 \\ \omega \mathbf{b}_3 &= \mathbf{b}_1 + \mathbf{b}_2 + \mathbf{b}_3 + \mathbf{b}_4 \\ \omega \mathbf{b}_4 &= -2\mathbf{b}_1 - 2\mathbf{b}_2 - 2\mathbf{b}_3 - \mathbf{b}_4. \end{aligned} \quad (49)$$

The \mathbf{b}_i are of unequal size and thus not appropriate for the approach outlined in section 2.2. It is therefore useful to define

$$\begin{aligned} \mathbf{e}_1 &= \mathbf{b}_1 \\ \mathbf{e}_2 &= \mathbf{b}_2 \\ \mathbf{e}_3 &= \mathbf{b}_3 \\ \mathbf{e}_4 &= \mathbf{b}_1 + \mathbf{b}_2 + \mathbf{b}_3 + \mathbf{b}_4. \end{aligned} \quad (50)$$

The \mathbf{e}_i are of equal magnitude and by inspection generate the same lattice as \mathbf{b}_i . satisfy $\omega \mathbf{e}_i = \mathbf{e}_{i+1}$ for $i = 1, 2, 3$ and $\omega \mathbf{e}_4 = -\mathbf{e}_1$. By inspection, they generate the same lattice as the \mathbf{b}_i . Denoting the lattice vectors of B_2 by \mathbf{e}_A , \mathbf{e}_B , and normalising all basis vectors to unity, we then have

$$\begin{aligned} \omega \mathbf{e}_A &= \mathbf{e}_B & \omega \mathbf{e}_1 &= \mathbf{e}_2 & \omega \mathbf{e}_2 &= \mathbf{e}_3 \\ \omega \mathbf{e}_B &= -\mathbf{e}_A & \omega \mathbf{e}_3 &= \mathbf{e}_4 & \omega \mathbf{e}_4 &= -\mathbf{e}_1. \end{aligned} \quad (51)$$

$$g_{ij} = \mathbf{e}_i \cdot \mathbf{e}_j = \begin{pmatrix} 1 & 0 & 0 & 0 & 0 & 0 \\ 0 & 1 & 0 & 0 & 0 & 0 \\ 0 & 0 & 1 & -\frac{1}{2} & 0 & \frac{1}{2} \\ 0 & 0 & -\frac{1}{2} & 1 & -\frac{1}{2} & 0 \\ 0 & 0 & 0 & -\frac{1}{2} & 1 & -\frac{1}{2} \\ 0 & 0 & \frac{1}{2} & 0 & -\frac{1}{2} & 1 \end{pmatrix}. \quad (52)$$

The lattice vectors are shown in figure 4. The action of R is given by

$$\begin{aligned} \mathbf{e}_A &\leftrightarrow \mathbf{e}_B \\ \mathbf{e}_1 &\leftrightarrow \mathbf{e}_1 \\ \mathbf{e}_2 &\leftrightarrow -\mathbf{e}_4 \\ \mathbf{e}_3 &\leftrightarrow -\mathbf{e}_3. \end{aligned} \quad (53)$$

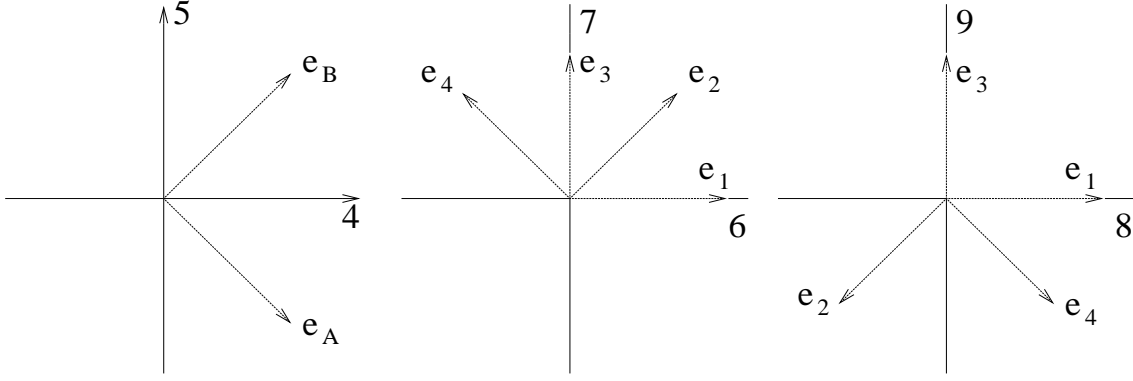


Figure 4: The \mathbb{Z}'_8 lattice

There are two independent insertions in the Klein bottle trace (6), ΩR and $\Omega R\Theta$. Under ΩR , the lattice modes in the untwisted sector are

$$\begin{aligned} \mathbf{p}_{\Omega R} &= l(\mathbf{e}_A + \mathbf{e}_B) + m(2\mathbf{e}_1) + n(\mathbf{e}_2 - \mathbf{e}_4), \quad l, m, n \in \mathbb{Z} \\ \mathbf{w}_{\Omega R} &= l'(\mathbf{e}_A - \mathbf{e}_B) + m'\mathbf{e}_3 + n(\mathbf{e}_2 + \mathbf{e}_4), \quad l', m', n' \in \mathbb{Z} \end{aligned} \quad (54)$$

and under $\Omega R\Theta$ we have

$$\begin{aligned} \mathbf{p}_{\Omega R\Theta} &= l\mathbf{e}_A + m(\mathbf{e}_1 - \mathbf{e}_4 + \mathbf{e}_2 - \mathbf{e}_3) + 2n(\mathbf{e}_1 - \mathbf{e}_4), \quad l, m, n \in \mathbb{Z} \\ \mathbf{w}_{\Omega R\Theta} &= l'\mathbf{e}_B + m'(\mathbf{e}_1 + \mathbf{e}_4) + n'(\mathbf{e}_2 + \mathbf{e}_3), \quad l', m', n' \in \mathbb{Z} \end{aligned} \quad (55)$$

From (54) we obtain

$$M_{KB, \Omega R} = \begin{pmatrix} 2 & 0 & 0 \\ 0 & 4 & -2 \\ 0 & -2 & 2 \end{pmatrix} \quad (56)$$

$$W_{KB, \Omega R} = \begin{pmatrix} 2 & 0 & 0 \\ 0 & 1 & -1 \\ 0 & -1 & 2 \end{pmatrix}. \quad (57)$$

Table 8: Fixed point structure for the $\mathbb{Z}'_8 B_2 \times B_4$ orbifold

	Fixed points	No. invariant under R	No. invariant under $R\Theta$
Θ	4	4	4
Θ^2	16	8	8
Θ^3	4	4	4
Θ^4	16	8	4

The lattice contribution in the untwisted sector for the ΩR insertion is then

$$\frac{64}{(\det M_{KB,\Omega R})^{\frac{1}{2}} (\det W_{KB,\Omega R})^{\frac{1}{2}}} = 16 \quad (58)$$

and it is easily verified that the $\Omega R\Theta$ insertion gives the same factor.

Lattice modes are also present in the Θ^4 twisted sector, which leaves the B_2 lattice invariant. In this case, the lattice contribution is

$$\frac{4}{(\det M)^{\frac{1}{2}} (\det W)^{\frac{1}{2}}} = \begin{cases} 2 & \Omega R \text{ insertion} \\ 4 & \Omega R\Theta \text{ insertion.} \end{cases} \quad (59)$$

For the twisted sectors, we also need to know the number of fixed points invariant under ΩR and $\Omega R\Theta$. In the Θ twisted sector, the B_2 lattice has by inspection one non-trivial fixed point, $\frac{1}{2}(\mathbf{e}_A + \mathbf{e}_B)$. In the B_4 lattice, fixed points under Θ satisfy

$$\omega(a_1\mathbf{e}_1 + a_2\mathbf{e}_2 + a_3\mathbf{e}_3 + a_4\mathbf{e}_4) \equiv a_1\mathbf{e}_1 + a_2\mathbf{e}_2 + a_3\mathbf{e}_3 + a_4\mathbf{e}_4 \quad (60)$$

where $a_i \equiv a_i + \mathbb{Z}$. This is solved to give $a_i = \frac{1}{2}$ as the one non-trivial solution. There are then a total of 4 Θ fixed points, having the form

$$\begin{pmatrix} \frac{1}{2} \\ 0 \end{pmatrix} (\mathbf{e}_A + \mathbf{e}_B) + \begin{pmatrix} \frac{1}{2} \\ 0 \end{pmatrix} (\mathbf{e}_1 + \mathbf{e}_2 + \mathbf{e}_3 + \mathbf{e}_4). \quad (61)$$

These are all invariant under the action of ΩR and $\Omega R\Theta$. In general, we calculate fixed points using our knowledge of the action of ω , and then use the action of ΩR to explicitly check which are invariant. The number of fixed points in the other twisted sectors is shown in table 8. As the Θ^{N-k} sector mirrors the Θ^k sector in its fixed point structure, we only show the first four twisted sectors.

Combining the lattice modes and the number of invariant fixed points, we can now evaluate the tree-channel Klein bottle amplitude

$$-c \int_0^\infty 16dl \left((\Theta^0) + 2(\Theta) + 4(\Theta^2) + 2(\Theta^3) - 4(\Theta^4) + 2(\Theta^5) - 4(\Theta^6) + 2(\Theta^7) \right). \quad (62)$$

We observe that equation (62) contains the complete projector.

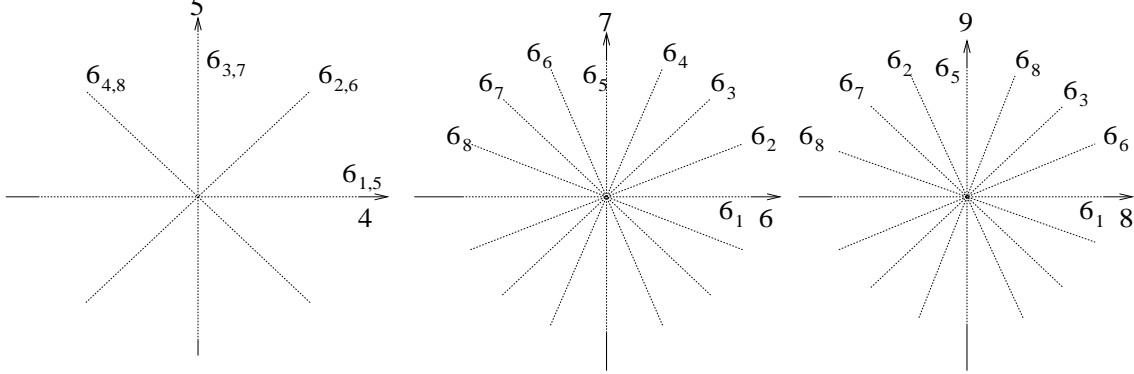


Figure 5: The \mathbb{Z}'_8 branes

Table 9: Brane intersection points

Sector	#	Location	Sector	#	Location
(1,2)	1	0	(2,3)	1	0
(1,3)	2	$(0, \frac{1}{2})(\mathbf{e}_A + \mathbf{e}_B)$	(2,4)	2	$(0, \frac{1}{2})(\mathbf{e}_1 + \mathbf{e}_2 + \mathbf{e}_3 + \mathbf{e}_4)$
(1,4)	1	0	(2,5)	1	0
(1,5)	2	$\frac{1}{2}(\mathbf{e}_2 - \mathbf{e}_4)$	(2,6)	4	$(0, \frac{1}{2})(\mathbf{e}_2 - \mathbf{e}_3) + (0, \frac{1}{2})(\mathbf{e}_1 - \mathbf{e}_4)$

D6-branes are then added as in figure 5, with M branes on each stack. There are two independent contributions to the annulus amplitude, coming from strings originating on the 6_{1+2n} and 6_{2n} branes. The 6_1 brane occupies the volume

$$\alpha(\mathbf{e}_A + \mathbf{e}_B) + \beta\mathbf{e}_1 + \gamma(\mathbf{e}_2 - \mathbf{e}_4) \quad (63)$$

so that

$$M_{A,11} = \begin{pmatrix} 2 & 0 & 0 \\ 0 & 1 & -1 \\ 0 & -1 & 2 \end{pmatrix}. \quad (64)$$

The lattice factor in the untwisted sector for $(6_1, 6_1)$ strings is then $\frac{(\det M_{A,11})}{(\det g)^{\frac{1}{2}}} = 4$. The 6_2 brane occupies the volume

$$\alpha'\mathbf{e}_B + \beta'(\mathbf{e}_1 + \mathbf{e}_2) + \gamma'(\mathbf{e}_3 - \mathbf{e}_4) \quad (65)$$

so that for $(6_2, 6_2)$ strings we likewise obtain a lattice factor of 4. In the Θ^4 ‘twisted’ sector, the $(6_1, 6_5)$ and $(6_2, 6_6)$ brane pairs coincide along the first torus. Here the lattice modes give a factor of 2 for $(6_1, 6_5)$ strings and 1 for $(6_2, 6_6)$ strings.

The intersection numbers can be computed as described in section 2.2 and are listed in table 9 together with their locations. The locations are necessary for

the Möbius strip amplitude and must be found by explicit computation, e.g. to find $(6_1, 6_2)$ intersection points we look for non-trivial solutions of

$$\alpha(\mathbf{e}_A + \mathbf{e}_B) + \beta\mathbf{e}_1 + \gamma(\mathbf{e}_2 - \mathbf{e}_4) \equiv \alpha'\mathbf{e}_B + \beta'(\mathbf{e}_1 + \mathbf{e}_2) + \gamma'(\mathbf{e}_3 - \mathbf{e}_4). \quad (66)$$

We can now write down the annulus amplitude

$$-cM^2 \int l dl \left(\frac{1}{16l^4}(\Theta^0)4 + \frac{1}{2l}(\Theta) + \frac{1}{2l}2(\Theta^2) + \frac{1}{2l}(\Theta^3) + \frac{l}{4l^2}4(\Theta^4) + \dots \right) \quad (67)$$

which can be brought to the form

$$A = -M^2 c \int \frac{dl}{4} ((\Theta^0) + 2(\Theta) + 4(\Theta^2) + 2(\Theta^3) - 4(\Theta^4) + \dots). \quad (68)$$

This has the same form as the Klein bottle amplitude (62).

For the Möbius amplitude, as discussed in section 2.2, we find

$$W_{MS,11} = W_{KB,\Omega R} = \begin{pmatrix} 2 & 0 & 0 \\ 0 & 1 & -1 \\ 0 & -1 & 2 \end{pmatrix} \quad (69)$$

$$M_{MS,11} = M_{A,11} = \begin{pmatrix} 2 & 0 & 0 \\ 0 & 1 & -1 \\ 0 & -1 & 2 \end{pmatrix}. \quad (70)$$

The lattice factor for $(6_1, 6_1)$ strings is then $64 \frac{(\det M_{MS,11})^{\frac{1}{2}}}{(\det W_{MS,11})^{\frac{1}{2}}} = 64$ and a similar treatment for $(6_2, 6_2)$ strings yields 64, as well.

No other lattice modes contribute to the Möbius amplitude. The 6_1 and 6_5 branes have a coincident direction and so could in principle have lattice modes. However, $(6_1, 6_5)$ strings are invariant under an insertion of $\Omega R \Theta^2$ in the trace. As this acts as a reflection on the coincident direction, there are no invariant lattice modes. Finally, all intersection points are invariant under the appropriate insertion of $\Omega R \Theta^k$ except those in the $(6_2, 6_6)$ sector. Here, only two of the four points are invariant.

We then obtain the following tree channel Möbius strip amplitude

$$Mc \int 4dl ((\Theta^0) + 2(\Theta) + 4(\Theta^2) + 2(\Theta^3) - 4(\Theta^4) + \dots). \quad (71)$$

To obtain (71) we have fixed the action of the various Chan-Paton matrices; this determines the open string spectrum. Extracting the leading divergence from the three amplitudes, we get

$$(M - 8)^2 = 0 \quad (72)$$

implying that we need stacks of 8 D-branes to cancel tadpoles and that the gauge group is $U(4) \times U(4)$.

The above represents a **BA** ΩR implementation. We can also consider the **AA** ΩR orientation. The tree channel Klein bottle amplitude is then

$$K = -c \int_0^\infty dl \left((16+4)(\Theta^0) + 8(2+2)(\Theta) + 8(8+2)(\Theta^2) + 8(2+2)(\Theta^3) - 8(8+2)(\Theta^4) + \dots \right) \quad (73)$$

Supposing that there are M 6_{2k} and N 6_{2k+1} branes, the tree channel annulus amplitude takes the form

$$A = -c \int \frac{dl}{32} \left((2M^2 + 8N^2)(\Theta^0) + 16MN(\Theta) + 8(M^2 + 4N^2)(\Theta^2) + 16MN(\Theta^3) - 8(M^2 + 4N^2)(\Theta^4) + \dots \right) \quad (74)$$

and the Möbius amplitude is similarly seen to be

$$M = c \int 4dl \left(\frac{1}{2}(M+N)(\Theta^0) + \frac{1}{2}(M+4N)(\Theta) + 2(M+N)(\Theta^2) + \frac{1}{2}(M+4N)(\Theta^3) - 2(M+N)(\Theta^4) + \dots \right). \quad (75)$$

The tadpole cancellation conditions imply $M = 16, N = 4$. This means that the gauge group is $U(8) \times U(2)$. The open string spectra for the two orientations are shown in Table 10.

Table 10: The \mathbb{Z}'_8 open string spectra

Sector	$\mathbb{Z}'_8(\mathbf{AA})$	$\mathbb{Z}'_8(\mathbf{BA})$
$(6_i, 6_i)$	$(1V + 1C) (\mathbf{64}, \mathbf{1}) \oplus (\mathbf{1}, \mathbf{4}) + 2C (\mathbf{28}, \mathbf{1}_0) \oplus (\overline{\mathbf{28}}, \mathbf{1}_0) \oplus (\mathbf{1}, \mathbf{1}) \oplus (\mathbf{1}, \overline{\mathbf{1}})$	$(1V + 1C) (\mathbf{16}, \mathbf{1}) \oplus (\mathbf{1}, \mathbf{16}) + 2C (\mathbf{6}, \mathbf{1}_0) \oplus (\overline{\mathbf{6}}, \mathbf{1}_0) \oplus (\mathbf{1}, \mathbf{6}) \oplus (\mathbf{1}, \overline{\mathbf{6}})$
$(6_i, 6_{i\pm 1})$	$1C (\mathbf{8}, \mathbf{2}) \oplus (\overline{\mathbf{8}}, \mathbf{2})$	$1C (\mathbf{4}, \mathbf{4}) \oplus (\overline{\mathbf{4}}, \mathbf{4})$
$(6_i, 6_{i\pm 2})$	$1C (\mathbf{28}, \mathbf{1}_0) \oplus (\overline{\mathbf{28}}, \mathbf{1}_0) + 4C (\mathbf{1}, \mathbf{1}) \oplus (\mathbf{1}, \overline{\mathbf{1}})$	$2C (\mathbf{6}, \mathbf{1}) \oplus (\overline{\mathbf{6}}, \mathbf{1}) \oplus (\mathbf{1}, \mathbf{6}) \oplus (\mathbf{1}, \overline{\mathbf{6}})$
$(6_i, 6_{i\pm 3})$	$1C (\mathbf{8}, \mathbf{2}) \oplus (\overline{\mathbf{8}}, \mathbf{2})$	$1C (\mathbf{4}, \mathbf{4}) \oplus (\overline{\mathbf{4}}, \mathbf{4})$
$(6_i, 6_{i+4})$	$2C (\mathbf{64}, \mathbf{1}_0) + 4C (\mathbf{1}, \mathbf{4})$	$2C (\mathbf{16}, \mathbf{1}) + 4C (\mathbf{1}, \mathbf{16})$

5.3 \mathbb{Z}_8 Model: $D_2 \times B_4$ with $v = \frac{1}{8}(-4, 1, 3)$

The \mathbb{Z}_8 lattice is very similar to the \mathbb{Z}'_8 lattice, the only difference being the replacement of B_2 by D_2 . Indeed, the lattice picture is a simple modification of

4. The action of ω on the lattice basis \mathbf{e}_i is

$$\begin{aligned}\omega \mathbf{e}_A &= -\mathbf{e}_A & \omega \mathbf{e}_1 &= \mathbf{e}_2 & \omega \mathbf{e}_2 &= \mathbf{e}_3 \\ \omega \mathbf{e}_B &= -\mathbf{e}_B & \omega \mathbf{e}_3 &= \mathbf{e}_4 & \omega \mathbf{e}_4 &= -\mathbf{e}_1.\end{aligned}\tag{76}$$

Here $\mathbf{e}_A, \mathbf{e}_B$ are a basis for the D_2 and the $\mathbf{e}_i, i = 1, \dots, 4$ are a basis for B_4 , as in section 5.2. The lattice metric for this basis is given by (52). In the same manner as in 5.2 we obtain consistent models for the two inequivalent ΩR implementations. The calculations are very similar to the \mathbb{Z}_8 orientifold. Gauge groups turn out to be $U(8) \times U(4)$ (**AA** case) and $U(4) \times U(2)$ (**BA** case). Results for open spectra are shown in Table 11.

Table 11: The \mathbb{Z}_8 open string spectra

Sector	$\mathbb{Z}_8(\mathbf{AA})$	$\mathbb{Z}_8(\mathbf{BA})$
$(6_i, 6_i)$	$(1V + 1C) (\mathbf{64}, \mathbf{1}) \oplus (\mathbf{1}, \mathbf{16}) +$ $2C (\mathbf{28}, \mathbf{1}) \oplus (\overline{\mathbf{28}}, \mathbf{1}) \oplus (\mathbf{1}, \mathbf{6}) \oplus (\mathbf{1}, \overline{\mathbf{6}})$	$(1V + 1C) (\mathbf{16}, \mathbf{1}) \oplus (\mathbf{1}, \mathbf{4}) +$ $2C (\mathbf{6}, \mathbf{1}_0) \oplus (\overline{\mathbf{6}}, \mathbf{1}_0) \oplus (\mathbf{1}_0, \mathbf{1}) \oplus (\mathbf{1}_0, \overline{\mathbf{1}})$
$(6_i, 6_{i\pm 1})$	$1C (\mathbf{8}, \overline{\mathbf{4}}) \oplus (\overline{\mathbf{8}}, \mathbf{4})$	$2C (\mathbf{4}, \overline{\mathbf{2}}) \oplus (\overline{\mathbf{4}}, \mathbf{2})$
$(6_i, 6_{i\pm 2})$	$2C (\mathbf{64}, \mathbf{1}) + 4C (\mathbf{1}, \mathbf{16})$	$2C (\mathbf{16}, \mathbf{1}) + 4C (\mathbf{1}, \mathbf{4})$
$(6_i, 6_{i\pm 3})$	$2C (\mathbf{8}, \overline{\mathbf{4}}) \oplus (\overline{\mathbf{8}}, \mathbf{4})$	$4C (\mathbf{4}, \overline{\mathbf{2}}) \oplus (\overline{\mathbf{4}}, \mathbf{2})$
$(6_i, 6_{i+4})$	$2C (\mathbf{28}, \mathbf{1}) \oplus (\overline{\mathbf{28}}, \mathbf{1}) + 4C (\mathbf{1}, \mathbf{6}) \oplus (\mathbf{1}, \overline{\mathbf{6}})$	$2C (\mathbf{6}, \mathbf{1}) \oplus (\overline{\mathbf{6}}, \mathbf{1}) + 4C (\mathbf{1}_0, \mathbf{1}) \oplus (\mathbf{1}_0, \overline{\mathbf{1}})$

5.4 \mathbb{Z}_{12} Model: $A_2 \times F_4$ with $v = \frac{1}{12}(4, 1, -5)$

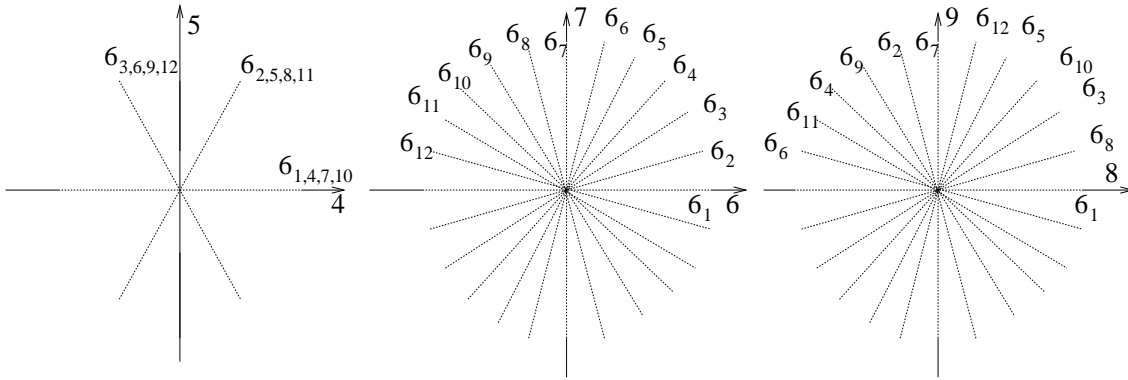


Figure 6: The $\mathbb{Z}_{12}(\mathbf{AA})$ branes

Here the lattice vectors are visualised as in figure 1, and the branes are placed as in figure 6. The action of ω on the lattice basis \mathbf{e}_i is given by

$$\begin{aligned} \omega \mathbf{e}_1 &= \mathbf{e}_2 & \omega \mathbf{e}_2 &= -(\mathbf{e}_1 + \mathbf{e}_2) & \omega \mathbf{e}_3 &= \mathbf{e}_4 \\ \omega \mathbf{e}_4 &= \mathbf{e}_5 & \omega \mathbf{e}_5 &= \mathbf{e}_6 & \omega \mathbf{e}_6 &= \mathbf{e}_5 - \mathbf{e}_3. \end{aligned} \quad (77)$$

and also

$$g_{ij} = \mathbf{e}_i \cdot \mathbf{e}_j = \begin{pmatrix} 1 & -\frac{1}{2} & 0 & 0 & 0 & 0 \\ -\frac{1}{2} & 1 & 0 & 0 & 0 & 0 \\ 0 & 0 & 1 & -\frac{1}{2} & \frac{1}{2} & 0 \\ 0 & 0 & -\frac{1}{2} & 1 & -\frac{1}{2} & \frac{1}{2} \\ 0 & 0 & \frac{1}{2} & -\frac{1}{2} & 1 & -\frac{1}{2} \\ 0 & 0 & 0 & \frac{1}{2} & -\frac{1}{2} & 1 \end{pmatrix} \quad (78)$$

The calculation follows exactly the same pattern as outlined above for the \mathbb{Z}'_8 case, and we find the tadpole cancellation condition

$$(M - 4)^2 = 0 \quad (79)$$

which implies a $U(2) \times U(2)$ gauge group. In this case there are two consistent implementations of ΩR . If we rotate the A_2 into a \mathbf{B} type lattice, then the effect is to multiply all the amplitudes by 3 which does not modify the tadpole cancellation conditions. We denote this model by $\mathbb{Z}_{12}(\mathbf{BA})$. The spectra for the two models are shown in table 12.

Table 12: The \mathbb{Z}_{12} open string spectra

Sector	$\mathbb{Z}_{12}(\mathbf{AA})$	$\mathbb{Z}_{12}(\mathbf{BA})$
$(6_i, 6_i)$	$(1V + 1C) (\mathbf{4}, \mathbf{1}) \oplus (\mathbf{1}, \mathbf{4}) +$ $2C (\mathbf{1}, \mathbf{1}_0) \oplus (\bar{\mathbf{1}}, \mathbf{1}_0) \oplus (\mathbf{1}_0, \mathbf{1}) \oplus (\mathbf{1}_0, \bar{\mathbf{1}})$	$(1V + 1C) (\mathbf{4}, \mathbf{1}) \oplus (\mathbf{1}, \mathbf{4}) +$ $2C (\mathbf{1}, \mathbf{1}_0) \oplus (\bar{\mathbf{1}}, \mathbf{1}_0) \oplus (\mathbf{1}_0, \mathbf{1}) \oplus (\mathbf{1}_0, \bar{\mathbf{1}})$
$(6_i, 6_{i\pm 1})$	$1C (\mathbf{2}, \bar{\mathbf{2}}) \oplus (\bar{\mathbf{2}}, \mathbf{2})$	$3C (\mathbf{2}, \bar{\mathbf{2}}) \oplus (\bar{\mathbf{2}}, \mathbf{2})$
$(6_i, 6_{i\pm 2})$	$1C (\mathbf{1}, \mathbf{1}_0) \oplus (\bar{\mathbf{1}}, \mathbf{1}_0) \oplus (\mathbf{1}_0, \mathbf{1}) \oplus (\mathbf{1}_0, \bar{\mathbf{1}})$	$3C (\mathbf{1}, \mathbf{1}_0) \oplus (\bar{\mathbf{1}}, \mathbf{1}_0) \oplus (\mathbf{1}_0, \mathbf{1}) \oplus (\mathbf{1}_0, \bar{\mathbf{1}})$
$(6_i, 6_{i\pm 3})$	$2C (\mathbf{2}, \bar{\mathbf{2}}) \oplus (\bar{\mathbf{2}}, \mathbf{2})$	$6C (\mathbf{2}, \bar{\mathbf{2}}) \oplus (\bar{\mathbf{2}}, \mathbf{2})$
$(6_i, 6_{i\pm 4})$	$2C (\mathbf{4}, \mathbf{1}) \oplus (\mathbf{1}, \mathbf{4}) +$ $1C (\mathbf{3}, \mathbf{1}) \oplus (\bar{\mathbf{3}}, \mathbf{1}) \oplus (\mathbf{1}, \mathbf{3}) \oplus (\mathbf{1}, \bar{\mathbf{3}})$	$6C (\mathbf{4}, \mathbf{1}) \oplus (\mathbf{1}, \mathbf{4}) +$ $3C (\mathbf{3}, \mathbf{1}) \oplus (\bar{\mathbf{3}}, \mathbf{1}) \oplus (\mathbf{1}, \mathbf{3}) \oplus (\mathbf{1}, \bar{\mathbf{3}})$
$(6_i, 6_{i\pm 5})$	$1C (\mathbf{2}, \bar{\mathbf{2}}) \oplus (\bar{\mathbf{2}}, \mathbf{2})$	$3C (\mathbf{2}, \bar{\mathbf{2}}) \oplus (\bar{\mathbf{2}}, \mathbf{2})$
$(6_i, 6_{i+6})$	$3C (\mathbf{1}, \mathbf{1}_0) \oplus (\bar{\mathbf{1}}, \mathbf{1}_0) \oplus (\mathbf{1}_0, \mathbf{1}) \oplus (\mathbf{1}_0, \bar{\mathbf{1}})$ $1C (\mathbf{3}, \mathbf{1}) \oplus (\bar{\mathbf{3}}, \mathbf{1}) \oplus (\mathbf{1}, \mathbf{3}) \oplus (\mathbf{1}, \bar{\mathbf{3}})$	$9C (\mathbf{1}, \mathbf{1}_0) \oplus (\bar{\mathbf{1}}, \mathbf{1}_0) \oplus (\mathbf{1}_0, \mathbf{1}) \oplus (\mathbf{1}_0, \bar{\mathbf{1}})$ $3C (\mathbf{3}, \mathbf{1}) \oplus (\bar{\mathbf{3}}, \mathbf{1}) \oplus (\mathbf{1}, \mathbf{3}) \oplus (\mathbf{1}, \bar{\mathbf{3}})$

We note that the different zero point energies of the twisted sectors result in the $\mathbf{A} + \bar{\mathbf{A}}$, $\mathbf{S} + \bar{\mathbf{S}}$, and \mathbf{Adj} representations appearing in the various sectors.

5.5 \mathbb{Z}'_{12} Model: $D_2 \times F_4$ with $v = \frac{1}{12}(-6, 1, 5)$

The \mathbb{Z}'_{12} case is very similar to the \mathbb{Z}_{12} case, the difference being the replacement of the A_2 by D_2 . The lattice vectors and brane positions are a simple modification of figures 1 and 6. The action of ω on the basis vectors \mathbf{e}_i for the lattice is:

$$\begin{aligned} \omega \mathbf{e}_1 &= -\mathbf{e}_1 & \omega \mathbf{e}_2 &= -\mathbf{e}_2 & \omega \mathbf{e}_3 &= \mathbf{e}_4 \\ \omega \mathbf{e}_4 &= \mathbf{e}_5 & \omega \mathbf{e}_5 &= \mathbf{e}_6 & \omega \mathbf{e}_6 &= \mathbf{e}_5 - \mathbf{e}_3 \end{aligned} \quad (80)$$

and the metric on the lattice is

$$g_{ij} = \mathbf{e}_i \cdot \mathbf{e}_j = \begin{pmatrix} 1 & 0 & 0 & 0 & 0 & 0 \\ 0 & 1 & 0 & 0 & 0 & 0 \\ 0 & 0 & 1 & -\frac{1}{2} & \frac{1}{2} & 0 \\ 0 & 0 & -\frac{1}{2} & 1 & -\frac{1}{2} & \frac{1}{2} \\ 0 & 0 & \frac{1}{2} & -\frac{1}{2} & 1 & -\frac{1}{2} \\ 0 & 0 & 0 & \frac{1}{2} & -\frac{1}{2} & 1 \end{pmatrix}. \quad (81)$$

Again, there are two consistent implementations of ΩR , arising from reorienting the D_2 lattice. This time the tadpole cancellation conditions are altered, the **AA** type lattice giving

$$(M - 8)^2 = 0 \quad (82)$$

and the **BA** type lattice giving

$$(M - 4)^2 = 0. \quad (83)$$

The spectra for the two models are shown in table 13.

Table 13: The \mathbb{Z}'_{12} open string spectra

Sector	$\mathbb{Z}'_{12}(\mathbf{AA})$	$\mathbb{Z}'_{12}(\mathbf{BA})$
$(6_i, 6_i)$	$(1V + 1C) (\mathbf{16}, \mathbf{1}) \oplus (\mathbf{1}, \mathbf{16}) +$ $2C (\mathbf{6}, \mathbf{1}) \oplus (\overline{\mathbf{6}}, \mathbf{1}) \oplus (\mathbf{1}, \mathbf{6}) \oplus (\mathbf{1}, \overline{\mathbf{6}})$	$(1V + 1C) (\mathbf{4}, \mathbf{1}) \oplus (\mathbf{1}, \mathbf{4}) +$ $2C (\mathbf{1}, \mathbf{1}_0) \oplus (\overline{\mathbf{1}}, \mathbf{1}_0) \oplus (\mathbf{1}_0, \mathbf{1}) \oplus (\mathbf{1}_0, \overline{\mathbf{1}})$
$(6_i, 6_{i\pm 1})$	$1C (\mathbf{4}, \overline{\mathbf{4}}) \oplus (\overline{\mathbf{4}}, \mathbf{4})$	$2C (\mathbf{2}, \overline{\mathbf{2}}) \oplus (\overline{\mathbf{2}}, \mathbf{2})$
$(6_i, 6_{i\pm 2})$	$2C (\mathbf{16}, \mathbf{1}) \oplus (\mathbf{1}, \mathbf{16})$	$2C (\mathbf{4}, \mathbf{1}) \oplus (\mathbf{1}, \mathbf{4})$
$(6_i, 6_{i\pm 3})$	$2C (\mathbf{4}, \overline{\mathbf{4}}) \oplus (\overline{\mathbf{4}}, \mathbf{4})$	$4C (\mathbf{2}, \overline{\mathbf{2}}) \oplus (\overline{\mathbf{2}}, \mathbf{2})$
$(6_i, 6_{i\pm 4})$	$2C (\mathbf{16}, \mathbf{1}) \oplus (\mathbf{1}, \mathbf{16}) +$ $4C (\mathbf{6}, \mathbf{1}) \oplus (\overline{\mathbf{6}}, \mathbf{1}) \oplus (\mathbf{1}, \mathbf{6}) \oplus (\mathbf{1}, \overline{\mathbf{6}})$	$2C (\mathbf{4}, \mathbf{1}) \oplus (\mathbf{1}, \mathbf{4}) +$ $4C (\mathbf{1}, \mathbf{1}_0) \oplus (\overline{\mathbf{1}}, \mathbf{1}_0) \oplus (\mathbf{1}_0, \mathbf{1}) \oplus (\mathbf{1}_0, \overline{\mathbf{1}})$
$(6_i, 6_{i\pm 5})$	$1C (\mathbf{4}, \overline{\mathbf{4}}) \oplus (\overline{\mathbf{4}}, \mathbf{4})$	$2C (\mathbf{2}, \overline{\mathbf{2}}) \oplus (\overline{\mathbf{2}}, \mathbf{2})$
$(6_i, 6_{i+6})$	$4C (\mathbf{16}, \mathbf{1}) \oplus (\mathbf{1}, \mathbf{16})$	$4C (\mathbf{4}, \mathbf{1}) \oplus (\mathbf{1}, \mathbf{4})$

5.6 \mathbb{Z}_4 Model: $A_3 \times A_3$ with $v = \frac{1}{4}(1, -2, 1)$

In table 2, many of the orbifolds have non-trivial fixed tori in some twisted sectors. These are contained inside one of the constituent lattices. For example, the \mathbb{Z}_{12} model on the E_6 lattice has a non-trivial fixed torus in the Θ^4 twisted sector. In such twisted sectors, we encounter many novel features. For example, the closed string winding modes may now be fractional multiples of lattice vectors. Nonetheless, after all issues are taken into account we still obtain perfect sector-by-sector tadpole cancellation. We will illustrate this by studying in detail the \mathbb{Z}_4 orientifold on the $A_3 \times A_3$ lattice. For compactness, we will only explicitly perform the calculations in the Θ^2 sector where there is a non-trivial fixed torus. The calculations in the other sectors are analogous to those studied above and neither present nor result in problems.

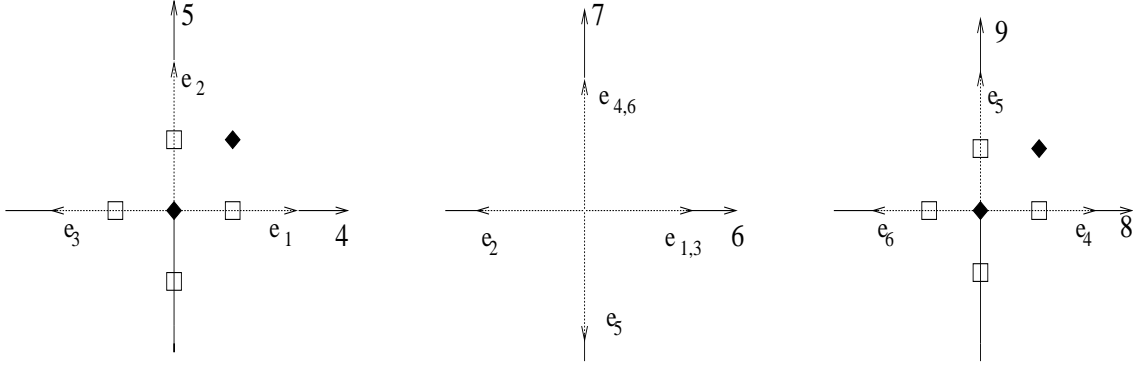


Figure 7: The $A_3 \times A_3$ \mathbb{Z}_4 vectors. The black dots represent the locations of Θ^2 fixed tori and the squares the loci for half-integral winding modes.

We can draw the $A_3 \times A_3$ lattice as in figure 7. The action of ω is

$$\begin{aligned} \omega \mathbf{e}_1 &= \mathbf{e}_2 & \omega \mathbf{e}_2 &= \mathbf{e}_3 & \omega \mathbf{e}_3 &= -\mathbf{e}_1 - \mathbf{e}_2 - \mathbf{e}_3 \\ \omega \mathbf{e}_4 &= \mathbf{e}_5 & \omega \mathbf{e}_5 &= \mathbf{e}_6 & \omega \mathbf{e}_6 &= -\mathbf{e}_4 - \mathbf{e}_5 - \mathbf{e}_6 \end{aligned} \quad (84)$$

and the metric is given by

$$g_{ij} = \mathbf{e}_i \cdot \mathbf{e}_j = \begin{pmatrix} 1 & -\frac{1}{2} & 0 & 0 & 0 & 0 \\ -\frac{1}{2} & 1 & -\frac{1}{2} & 0 & 0 & 0 \\ 0 & -\frac{1}{2} & 1 & 0 & 0 & 0 \\ 0 & 0 & 0 & 1 & -\frac{1}{2} & 0 \\ 0 & 0 & 0 & -\frac{1}{2} & 1 & -\frac{1}{2} \\ 0 & 0 & 0 & 0 & -\frac{1}{2} & 1 \end{pmatrix}. \quad (85)$$

There are three independent implementations of R : **AAA**, **BAA** and **AAB**. Here **A** and **B** denote the orientation of the R fixed plane in each rotation plane;

A corresponds to aligning the fixed plane along the x -axis and **B** at an angle of $\frac{\pi}{4}$ to this. In case **AAA** R acts as

$$\begin{aligned}
\mathbf{e}_1 &\leftrightarrow \mathbf{e}_1 \\
\mathbf{e}_2 &\leftrightarrow -\mathbf{e}_1 - \mathbf{e}_2 - \mathbf{e}_3 \\
\mathbf{e}_3 &\leftrightarrow \mathbf{e}_3 \\
\mathbf{e}_4 &\leftrightarrow -\mathbf{e}_6 \\
\mathbf{e}_5 &\leftrightarrow -\mathbf{e}_5
\end{aligned} \tag{86}$$

and in case **BAA** the action is

$$\begin{aligned}
\mathbf{e}_1 &\leftrightarrow \mathbf{e}_1 + \mathbf{e}_2 + \mathbf{e}_3 \\
\mathbf{e}_2 &\leftrightarrow -\mathbf{e}_3 \\
\mathbf{e}_4 &\leftrightarrow -\mathbf{e}_6 \\
\mathbf{e}_5 &\leftrightarrow -\mathbf{e}_5
\end{aligned} \tag{87}$$

and finally in case **AAB** R acts as

$$\begin{aligned}
\mathbf{e}_1 &\leftrightarrow \mathbf{e}_1 \\
\mathbf{e}_2 &\leftrightarrow -\mathbf{e}_1 - \mathbf{e}_2 - \mathbf{e}_3 \\
\mathbf{e}_3 &\leftrightarrow \mathbf{e}_3 \\
\mathbf{e}_4 &\leftrightarrow \mathbf{e}_5 \\
\mathbf{e}_6 &\leftrightarrow -\mathbf{e}_4 - \mathbf{e}_5 - \mathbf{e}_6.
\end{aligned} \tag{88}$$

We will only explicitly consider the **AAA** ΩR orientation, as the behaviour for **BAA** and **AAB** is similar. For the Klein bottle amplitude, we need to know the structure of fixed points and fixed tori. The Θ^2 sector has 4 fixed tori

$$\frac{n'}{2}(\mathbf{e}_1 + \mathbf{e}_2) + \frac{m'}{2}(\mathbf{e}_4 + \mathbf{e}_5) + \alpha(\mathbf{e}_1 + \mathbf{e}_3) + \beta(\mathbf{e}_4 + \mathbf{e}_6) \tag{89}$$

where $n', m' \in \{0, 1\}$. From figure 7, or by explicit computation, one can see that the action of R on the fixed tori in general involves a shift as well as a reflection. As the lattice is non-factorisable, the different rotation planes do not decouple from each other.

In the Θ^2 twisted sector, naively the momentum and winding modes would be, for an ΩR insertion in the trace,

$$\begin{aligned}
\mathbf{p} &= \frac{n}{2}(\mathbf{e}_1 + \mathbf{e}_3) \\
\mathbf{w} &= m(\mathbf{e}_4 + \mathbf{e}_6)
\end{aligned} \tag{90}$$

with $m, n \in \mathbb{Z}$, and for an $\Omega R\Theta$ insertion in the trace,

$$\begin{aligned}
\mathbf{p} &= \frac{n}{2}(\mathbf{e}_4 + \mathbf{e}_6) \\
\mathbf{w} &= m(\mathbf{e}_1 + \mathbf{e}_3).
\end{aligned} \tag{91}$$

However, there are two subtle issues that render this invalid. First, since R acts as

$$\begin{aligned} R : \frac{1}{2}(\mathbf{e}_1 + \mathbf{e}_2) &\rightarrow \frac{1}{2}(\mathbf{e}_1 + \mathbf{e}_2) + \frac{1}{2}(\mathbf{e}_1 + \mathbf{e}_3) \\ R : \frac{1}{2}(\mathbf{e}_4 + \mathbf{e}_5) &\rightarrow \frac{1}{2}(\mathbf{e}_4 + \mathbf{e}_5) + \frac{1}{2}(\mathbf{e}_4 + \mathbf{e}_6), \end{aligned} \quad (92)$$

on the fixed tori labelled by (n', m') R acts as a shift by $\frac{n'}{2}(\mathbf{e}_1 + \mathbf{e}_3) + \frac{m'}{2}(\mathbf{e}_4 + \mathbf{e}_6)$. Recall that the effect of a translation $T : \mathbf{x} \rightarrow \mathbf{x} + \mathbf{a}$ on a momentum mode $|\mathbf{p}\rangle$ is

$$T|\mathbf{p}\rangle = \exp(2\pi i \mathbf{p} \cdot \mathbf{a})|\mathbf{p}\rangle. \quad (93)$$

Therefore, for tori where $n' = 1$, momentum modes having $\mathbf{p} = (1 + 2k)(\mathbf{e}_1 + \mathbf{e}_3)$ pick up a phase factor of $e^{i\pi}$ under the action of R . When the sum over momentum modes is performed, such modes have no net contribution, because they cancel against similar modes from tori where no such shift occurs. This results in an effective doubling of the momentum modes. Schematically,

$$\sum_n (-1)^n \exp(-\pi t n^2 p^2) + \sum_n \exp(-\pi t n^2 p^2) = 2 \sum_n \exp(-4\pi t n^2 p^2). \quad (94)$$

The shift along the winding direction does not have any effect on the sum in the partition function. Moreover, as

$$\begin{aligned} R\Theta : \frac{1}{2}(\mathbf{e}_1 + \mathbf{e}_2) &\rightarrow \frac{1}{2}(\mathbf{e}_1 + \mathbf{e}_2) \\ R\Theta : \frac{1}{2}(\mathbf{e}_4 + \mathbf{e}_5) &\rightarrow \frac{1}{2}(\mathbf{e}_4 + \mathbf{e}_5) \end{aligned} \quad (95)$$

the insertion of $\Omega R\Theta$ has no effect on the contributing momentum modes.

There is also a subtlety at work for the winding modes. The condition that a string state be an acceptable orbifold state in the Θ^2 twisted sector is that

$$X^\mu(\sigma + 2\pi, \tau) = \Theta^2 X^\mu(\sigma, \tau). \quad (96)$$

Consider the points marked with a square in figure 7. These have the property that, when acted on with Θ^2 , they are brought back to themselves with a shift by either $\frac{1}{2}(\mathbf{e}_4 + \mathbf{e}_6)$ or $\frac{1}{2}(\mathbf{e}_1 + \mathbf{e}_3)$. Explicitly, we have for example

$$\Theta^2 \frac{1}{4}(\mathbf{e}_4 - \mathbf{e}_6) = \frac{1}{4}(\mathbf{e}_4 - \mathbf{e}_6) + \frac{1}{2}(\mathbf{e}_4 + \mathbf{e}_6) \quad (97)$$

It is this shift that allows the existence of winding modes that are half-integral multiples of lattice vectors. Thus the winding state

$$X(\sigma, \tau) = \frac{1}{4}(\mathbf{e}_4 - \mathbf{e}_6) + \frac{\sigma}{2\pi} \frac{(\mathbf{e}_4 + \mathbf{e}_6)}{2} + (\tau \text{ dependence}) \quad (98)$$

is a legitimate orbifold state in the Θ^2 twisted sector.

Next, we must consider whether these states are invariant under the action of ΩR and $\Omega R\Theta$. Under the insertion of $\Omega R\Theta$, all loci for half-integral winding modes are exchanged among themselves and there is no net contribution to the partition function. However, under the insertion of ΩR , four such loci survive, and we have additional winding modes of the form

$$X(\sigma, \tau) = \begin{pmatrix} \frac{1}{2} \\ 0 \end{pmatrix} (\mathbf{e}_1 + \mathbf{e}_2) \pm \frac{\mathbf{e}_4 - \mathbf{e}_6}{4} + \frac{\sigma}{2\pi} \frac{\mathbf{e}_4 + \mathbf{e}_6}{2} + (\tau \text{ dependence}). \quad (99)$$

The multiplicity is exactly the same as that of the number of fixed tori and the net effect is then that the effective winding mode for the ΩR insertion is reduced from $(\mathbf{e}_4 + \mathbf{e}_6)$ to $\frac{1}{2}(\mathbf{e}_4 + \mathbf{e}_6)$. For the $\Omega R\Theta$ insertion, the net winding mode is unchanged.

The actual momentum and winding modes appearing in the partition function are then, for an ΩR insertion in the trace

$$\begin{aligned} \mathbf{p} &= n(\mathbf{e}_1 + \mathbf{e}_3) \\ \mathbf{w} &= \frac{m}{2}(\mathbf{e}_4 + \mathbf{e}_6) \end{aligned} \quad (100)$$

with $m, n \in \mathbb{Z}$, and for an $\Omega R\Theta$ insertion in the trace,

$$\begin{aligned} \mathbf{p} &= \frac{n}{2}(\mathbf{e}_4 + \mathbf{e}_6) \\ \mathbf{w} &= m(\mathbf{e}_1 + \mathbf{e}_3). \end{aligned} \quad (101)$$

Performing a similar analysis for the other cases, we obtain the following Klein bottle amplitudes

$$\begin{aligned} \text{Case } \mathbf{AAA} & -c \int_0^\infty 16dl ((\Theta^0) + 4(\Theta) - 4(\Theta^2) - 4(\Theta^3)) \\ \text{Case } \mathbf{BAA} & -c \int_0^\infty 32dl ((\Theta^0) + 4(\Theta) - 4(\Theta^2) - 4(\Theta^3)) \\ \text{Case } \mathbf{AAB} & -c \int_0^\infty 8dl ((\Theta^0) + 4(\Theta) - 4(\Theta^2) - 4(\Theta^3)). \end{aligned} \quad (102)$$

Let us now consider the annulus amplitudes. We describe case **AAA** in detail and quote the results for the other cases. For case **AAA**, the branes are at

$$\begin{aligned} 6_1 & \alpha \mathbf{e}_1 + \beta \mathbf{e}_3 + \gamma(\mathbf{e}_4 - \mathbf{e}_6) \\ 6_2 & \alpha(\mathbf{e}_1 + \mathbf{e}_2) + \beta(\mathbf{e}_4 + \mathbf{e}_5) + \gamma(\mathbf{e}_4 + \mathbf{e}_6) \\ 6_3 & \alpha \mathbf{e}_2 + \beta(\mathbf{e}_1 + \mathbf{e}_3) + \gamma(2\mathbf{e}_5 + \mathbf{e}_4 + \mathbf{e}_6) \\ 6_4 & \alpha(\mathbf{e}_2 + \mathbf{e}_3) + \beta(\mathbf{e}_5 + \mathbf{e}_6) + \gamma(\mathbf{e}_4 + \mathbf{e}_6). \end{aligned} \quad (103)$$

As before, we focus on the sector arising from $(6_1, 6_3)$ and $(6_2, 6_4)$ strings. In each case there are two intersection points: 0 and $\frac{1}{2}(\mathbf{e}_4 + \mathbf{e}_6)$ for $(6_1, 6_3)$ strings and

0 and $\frac{1}{2}(\mathbf{e}_5 + \mathbf{e}_6)$ for $(6_2, 6_4)$ strings. For the former case, the lattice modes are given by

$$\begin{aligned}\mathbf{p} &= \frac{n}{2}(\mathbf{e}_1 + \mathbf{e}_3) \\ \mathbf{w} &= \frac{m}{2}(\mathbf{e}_4 + \mathbf{e}_6)\end{aligned}\tag{104}$$

and for $(6_2, 6_4)$ strings by

$$\begin{aligned}\mathbf{p} &= \frac{n}{2}(\mathbf{e}_4 + \mathbf{e}_6) \\ \mathbf{w} &= \frac{m}{2}(\mathbf{e}_1 + \mathbf{e}_3).\end{aligned}\tag{105}$$

Interestingly, the winding modes in the second case are a composite result of strings starting at two distinct points. The cases of m even arise from strings starting at $\mathbf{0}$; the cases of m odd arise from strings starting at $\frac{1}{2}(\mathbf{e}_1 + \mathbf{e}_2)$. Similar behaviour occurs for the other two cases. Computing the annulus amplitude, we obtain

$$\begin{aligned}\text{Case } \mathbf{AAA} & -cM^2 \int_0^\infty \frac{dl}{4} ((\Theta^0) + 4(\Theta) - 4(\Theta^2) - 4(\Theta^3)) \\ \text{Case } \mathbf{BAA} & -cM^2 \int_0^\infty \frac{dl}{2} ((\Theta^0) + 4(\Theta) - 4(\Theta^2) - 4(\Theta^3)) \\ \text{Case } \mathbf{AAB} & -cM^2 \int_0^\infty \frac{dl}{8} ((\Theta^0) + 4(\Theta) - 4(\Theta^2) - 4(\Theta^3)).\end{aligned}\tag{106}$$

In the computation of the Möbius strip amplitude, the Θ^2 sector arises from the insertion of $\Omega R \Theta^2$ into the trace, for $(6_1, 6_1)$ and $(6_2, 6_2)$ strings. This insertion leaves one plane invariant, which can then contribute lattice modes. The contributing modes are then, for case **AAA**,

$$\begin{aligned}(6_1, 6_1) \quad \mathbf{p} &= n(\mathbf{e}_1 + \mathbf{e}_3), \quad \mathbf{w} = \frac{m}{2}(\mathbf{e}_4 + \mathbf{e}_6) \\ (6_2, 6_2) \quad \mathbf{p} &= \frac{n}{2}(\mathbf{e}_4 + \mathbf{e}_6), \quad \mathbf{w} = m(\mathbf{e}_1 + \mathbf{e}_3).\end{aligned}\tag{107}$$

Here, new behaviour is seen for the winding modes in the $(6_1, 6_1)$ sector. For the factorisable models studied previously, half-integral winding modes did not appear in the Möbius strip amplitude. Instead, a winding mode doubling was observed. To see where the difference lies, consider the $(6_1, 6_1)$ winding mode starting at $\mathbf{0}$ and ending at $\frac{1}{2}(\mathbf{e}_4 - \mathbf{e}_6)$ and having winding vector $\frac{1}{2}(\mathbf{e}_4 + \mathbf{e}_6)$. Under $\Omega R \Theta^2$, this is taken to a winding mode which starts at $\frac{1}{2}(\mathbf{e}_4 - \mathbf{e}_6)$ and ends at $\mathbf{0}$, with the winding vector remaining invariant. So, the effect of $\Omega R \Theta^2$ on these modes is as a translation,

$$T : \mathbf{x} \rightarrow \mathbf{x} + \frac{1}{2}(\mathbf{e}_4 - \mathbf{e}_6).\tag{108}$$

As in (93), this causes momentum modes to pick up a phase $\exp(\pi i \mathbf{p} \cdot (\mathbf{e}_4 - \mathbf{e}_6))$. For the case above, the momentum modes are orthogonal to the translation direction and the phase factor is unity. Therefore the half-integral modes contribute to the partition function. In the factorisable case, the momentum modes lay along the translation direction. For half-integral winding modes, the sum of the momentum modes in the partition function was then

$$\sum_n (-1)^n \exp(-\pi t n^2 p^2) \quad (109)$$

which does not give rise to any divergence in the $t \rightarrow 0$ limit. This can be seen straightforwardly using the Poisson resummation formula. Having taken the above points into account, we obtain the following Möbius strip amplitudes

$$\begin{aligned} \text{Case AAA} \quad & cM \int_0^\infty 4dl ((\Theta^0) + 4(\Theta) - 4(\Theta^2) - 4(\Theta^3)) \\ \text{Case BAA} \quad & cM \int_0^\infty 8dl ((\Theta^0) + 4(\Theta) - 4(\Theta^2) - 4(\Theta^3)) \\ \text{Case AAB} \quad & cM \int_0^\infty 2dl ((\Theta^0) + 4(\Theta) - 4(\Theta^2) - 4(\Theta^3)). \end{aligned} \quad (110)$$

Comparing the respective Klein bottle, annulus and Möbius strip amplitudes, we see that in all three cases the amplitudes factorise perfectly and we obtain a tadpole cancellation condition

$$(M - 8)^2 = 0 \quad (111)$$

giving a gauge group of $U(4) \times U(4)$. The behaviour encountered above in the $A_3 \times A_3$ is typical of those models which have a non-trivial fixed torus in one of the twisted sectors. After taking into account the subtleties described above, and if necessary using different numbers of branes on different O-planes, one can cancel all tadpoles sector-by-sector. Despite the many subtleties involved in the one-loop calculation, at the end one obtains a simple answer. Indeed, for the $A_3 \times A_3$ case above the amplitudes actually take the form of the complete projector.

As well as the models written up in detail above, we have also studied all other cases in table 2. In table 14 we give tadpole-cancelling solutions for all ΩR orientations for the models in table 2. For cases 1,2,5 and 7, some results have already appeared in [6]. The spectra for these models can be determined exactly as for the other cases using the methods described in section 3. However, as they would not present any new features we have not written them out.

6 Conclusions

In this paper we have developed techniques to construct supersymmetric Type IIA orientifolds on six-dimensional orbifolds which do not factorise into three

Table 14: IIA Orientifolds of \mathbb{Z}_N orbifolds with D-branes on O-planes

Case	Lie algebra root lattice	ΩR orientation	No. of branes	Gauge Group
1 \mathbb{Z}_3	$A_2 \times A_2 \times A_2$	4 described in [6]	$M = 4$	$SO(4)$
2 \mathbb{Z}_4	$A_1 \times A_1 \times B_2 \times B_2$	AAA AAB ABA ABB	$M = 32, N = 8$ $M = 16, N = 4$ $M = 16, N = 16$ $M = 8, N = 8$	$U(16) \times U(4)$ $U(8) \times U(2)$ $U(8) \times U(8)$ $U(4) \times U(4)$
3 \mathbb{Z}_4	$A_1 \times A_3 \times B_2$	AAA ABA AAB ABB	$M=16, N=4$ $M = 16, N = 8$ $M = 8, N = 8$ $M = 8, N = 16$	$U(8) \times U(2)$ $U(8) \times U(4)$ $U(4) \times U(4)$ $U(4) \times U(8)$
4 \mathbb{Z}_4	$A_3 \times A_3$	AAA BAA AAB	$M = N = 8$ $M = N = 8$ $M = N = 8$	$U(4) \times U(4)$ $U(4) \times U(4)$ $U(4) \times U(4)$
5 \mathbb{Z}_6	$A_2 \times G_2 \times G_2$	AAA BBB ABA ABB	$M = N = 4$ $M = N = 4$ $M = N = 4$ $M = N = 4$	$U(2) \times U(2)$ $U(2) \times U(2)$ $U(2) \times U(2)$ $U(2) \times U(2)$
6 \mathbb{Z}_6	$G_2 \times A_2 \times A_2$	AA BA	$M = N = 4$ $M = N = 4$	$U(2) \times U(2)$ $U(2) \times U(2)$
7 \mathbb{Z}'_6	$A_1 \times A_1 \times A_2 \times G_2$	AAA AAB BBB ABB	$M = N = 4$ $M = N = 4$ $M = N = 4$ $M = N = 4$	$U(2) \times U(2)$ $U(2) \times U(2)$ $U(2) \times U(2)$ $U(2) \times U(2)$
9 \mathbb{Z}'_6	$A_1 \times A_1 \times A_2 \times A_2$	AA BA	$M = N = 8$ $M = N = 4$	$U(4) \times U(4)$ $U(2) \times U(2)$
10 \mathbb{Z}'_6	$A_1 \times A_5$	AAA AAB	$M = 8, N = 4$ $M = N = 8$	$U(4) \times U(2)$ $U(4) \times U(4)$
11 \mathbb{Z}_7	A_6	A B	$M = 4$ $M = 4$	$SO(4)$ $SO(4)$
12 \mathbb{Z}_8	$B_4 \times D_2$	AA BA	$M = 16, N = 8$ $M = 8, N = 4$	$U(8) \times U(4)$ $U(4) \times U(2)$
13 \mathbb{Z}_8	$A_1 \times D_5$	AA AB	$M = N = 8$ $M = N = 8$	$U(4) \times U(4)$ $U(4) \times U(4)$
14 \mathbb{Z}'_8	$B_2 \times B_4$	AA BA	$M = 16, N = 4$ $M = N = 8$	$U(8) \times U(2)$ $U(4) \times U(4)$
15 \mathbb{Z}'_8	$A_3 \times A_3$	A	$M = 8, N = 4$	$U(4) \times U(2)$
16 \mathbb{Z}_{12}	$A_2 \times F_4$	AA BA	$M = N = 4$ $M = N = 4$	$U(2) \times U(2)$ $U(2) \times U(2)$
17 \mathbb{Z}_{12}	E_6	A	$M = N = 4$	$U(2) \times U(2)$
18 \mathbb{Z}'_{12}	$D_2 \times F_4$	AA BA	$M = N = 4$ $M = N = 8$	$U(2) \times U(2)$ $U(2) \times U(2)$

two-dimensional tori. Using these techniques we have constructed many new explicit orientifold models, where we placed the D6-branes parallel to the orientifold planes. For some of these models, in particular those containing non-trivial fixed tori, we have encountered some new technical features in the amplitudes, which nicely played together to finally yield consistent solutions to the tadpole cancellation conditions. All these supersymmetric Type IIA orientifold models are expected to lift up to M-theory compactifications on singular compact G_2 manifolds [52, 53, 54].

The next step is to move beyond these simple solutions to the tadpole cancellation conditions and to study more general (supersymmetric) intersecting D-brane models in these backgrounds. It is expected that these more general intersecting D6-branes give rise to chirality and might be interesting for building semi-realistic models. Once interesting models are found, employing the results of the effective low energy action as described in [55, 56, 57, 58, 59, 60, 61, 62], the discussion of the phenomenological implications would be the natural next step to perform.

Acknowledgements

RB is supported by PPARC and JC is grateful to EPSRC for a research studentship. KS thanks Trinity College, Cambridge for financial support. It is a pleasure to thank Fernando Quevedo for helpful comments and encouragement.

A Oscillator Formulae

Here we give the oscillator contribution to the tree channel amplitude for a complex plane twisted by θ . For the closed string traces, this means that points related by a rotation of $2\pi\theta$ are identified. For the open string sectors, this refers to strings stretching between branes at a relative angle $\pi\theta$.

$$\begin{aligned}
\text{Klein bottle} \quad \theta = 0 & \quad \frac{1}{2l} \frac{\vartheta \left[\begin{smallmatrix} \frac{1}{2} \\ 0 \end{smallmatrix} \right]}{\eta^3} (2il) \\
|\theta| \in (0, \frac{1}{2}] & \quad \frac{\vartheta \left[\begin{smallmatrix} \frac{1}{2} \\ |\theta| \end{smallmatrix} \right]}{\vartheta \left[\begin{smallmatrix} \frac{1}{2} \\ |\theta| - \frac{1}{2} \end{smallmatrix} \right]} (2il) \\
\text{Annulus} \quad \theta = 0 & \quad \frac{1}{2l} \frac{\vartheta \left[\begin{smallmatrix} \frac{1}{2} \\ 0 \end{smallmatrix} \right]}{\eta^3} (2il) \\
|\theta| \in (0, \frac{1}{2}] & \quad \frac{\vartheta \left[\begin{smallmatrix} \frac{1}{2} \\ |\theta| \end{smallmatrix} \right]}{\vartheta \left[\begin{smallmatrix} \frac{1}{2} \\ |\theta| - \frac{1}{2} \end{smallmatrix} \right]} (2il)
\end{aligned} \tag{112}$$

$$\begin{aligned}
\text{Möbius strip} \quad \theta = 0 & \quad \frac{1}{4l} \frac{\vartheta \begin{bmatrix} \frac{1}{2} \\ 0 \end{bmatrix} \vartheta \begin{bmatrix} 0 \\ \frac{1}{2} \end{bmatrix}}{\eta^3 \vartheta \begin{bmatrix} 0 \\ 0 \end{bmatrix}} (4il) \\
|\theta| \in (0, \frac{1}{2}] & \quad \left(\frac{\vartheta \begin{bmatrix} \frac{1}{2} \\ \frac{|\theta|}{2} \end{bmatrix} \vartheta \begin{bmatrix} \frac{1}{2} \\ -\frac{|\theta|}{2} \end{bmatrix} \vartheta \begin{bmatrix} 0 \\ \frac{|\theta|}{2} - \frac{1}{2} \end{bmatrix} \vartheta \begin{bmatrix} 0 \\ \frac{1}{2} - \frac{|\theta|}{2} \end{bmatrix}}{\vartheta \begin{bmatrix} 0 \\ \frac{|\theta|}{2} \end{bmatrix} \vartheta \begin{bmatrix} 0 \\ -\frac{|\theta|}{2} \end{bmatrix} \vartheta \begin{bmatrix} \frac{1}{2} \\ \frac{|\theta|}{2} - \frac{1}{2} \end{bmatrix} \vartheta \begin{bmatrix} \frac{1}{2} \\ \frac{1}{2} - \frac{|\theta|}{2} \end{bmatrix}} (4il) \right)^{\frac{1}{2}} \\
\text{Möbius strip (2)} \quad \theta = 0 & \quad 2 \frac{\vartheta \begin{bmatrix} \frac{1}{2} \\ \frac{1}{2} \end{bmatrix} \vartheta \begin{bmatrix} 0 \\ 0 \end{bmatrix}}{\vartheta \begin{bmatrix} \frac{1}{2} \\ 0 \end{bmatrix} \vartheta \begin{bmatrix} 0 \\ \frac{1}{2} \end{bmatrix}} (4il) \\
|\theta| \in (0, \frac{1}{2}] & \quad \left(\frac{\vartheta \begin{bmatrix} 0 \\ \frac{|\theta|}{2} \end{bmatrix} \vartheta \begin{bmatrix} 0 \\ -\frac{|\theta|}{2} \end{bmatrix} \vartheta \begin{bmatrix} \frac{1}{2} \\ \frac{|\theta|}{2} - \frac{1}{2} \end{bmatrix} \vartheta \begin{bmatrix} \frac{1}{2} \\ \frac{1}{2} - \frac{|\theta|}{2} \end{bmatrix}}{\vartheta \begin{bmatrix} \frac{1}{2} \\ \frac{|\theta|}{2} \end{bmatrix} \vartheta \begin{bmatrix} \frac{1}{2} \\ -\frac{|\theta|}{2} \end{bmatrix} \vartheta \begin{bmatrix} 0 \\ \frac{|\theta|}{2} - \frac{1}{2} \end{bmatrix} \vartheta \begin{bmatrix} 0 \\ \frac{1}{2} - \frac{|\theta|}{2} \end{bmatrix}} (4il) \right)^{\frac{1}{2}}
\end{aligned}$$

For $(6_i, 6_{i+2k})$ strings, the two Möbius strip amplitudes correspond to the schematic insertions of $\Omega R \Theta^k$ and $\Omega R \Theta^{k+\frac{N}{2}}$. For odd orbifolds, only the former case is present. The former contributes to the Θ^k twisted sector; the latter to the $\Theta^{k+\frac{N}{2}}$ twisted sector.

The definitions of the ϑ functions can be found in the appendix of [6]. All the amplitudes were transformed to tree channel using the modular transformation properties

$$\begin{aligned}
\vartheta \begin{bmatrix} \alpha \\ \beta \end{bmatrix} (t^{-1}) &= \sqrt{t} e^{2\pi i \alpha \beta} \vartheta \begin{bmatrix} -\beta \\ \alpha \end{bmatrix} (t) \\
\eta(t^{-1}) &= \sqrt{t} \eta(t).
\end{aligned} \tag{113}$$

Explicitly writing out the oscillator contribution to the twisted amplitudes is neither interesting nor enlightening. We have throughout this paper used (Θ^k) to denote the appropriate combination of ϑ functions for the Θ^k twisted sector. In general this consists of a product of the above terms, one for each complex rotation plane. Where applicable, this also includes the sum of lattice modes $\sum_{n_i} \exp(-\pi l n_i (A)_{ij} n_j)$ that goes to 1 in the $l \rightarrow \infty$ limit. The leading numerical factors we always show explicitly. As an example, in the case of the \mathbb{Z}_7 annulus amplitude, (Θ^1) refers to the Θ twisted sector, and is given by

$$(\Theta^1) = \frac{\vartheta \begin{bmatrix} \frac{1}{2} \\ 0 \end{bmatrix} \vartheta \begin{bmatrix} \frac{1}{2} \\ \frac{1}{7} \end{bmatrix} \vartheta \begin{bmatrix} \frac{1}{2} \\ \frac{2}{7} \end{bmatrix} \vartheta \begin{bmatrix} \frac{1}{2} \\ \frac{3}{7} \end{bmatrix}}{\eta^3 \vartheta \begin{bmatrix} \frac{1}{2} \\ \frac{1}{7} - \frac{1}{2} \end{bmatrix} \vartheta \begin{bmatrix} \frac{1}{2} \\ \frac{2}{7} - \frac{1}{2} \end{bmatrix} \vartheta \begin{bmatrix} \frac{1}{2} \\ \frac{3}{7} - \frac{1}{2} \end{bmatrix}} (2il). \tag{114}$$

B Lattices

In this appendix we describe the various lattices in terms of the action of Θ on the basis vectors for the lattice on the three planes where Θ acts as a rotation. In every case, the picture describing the components of the basis vectors in each of the three planes, as well as the metric for that basis and the explicit action of Θ on the basis are given.

1. $\mathbb{Z}_3, \mathbf{A}_2 \times \mathbf{A}_2 \times \mathbf{A}_2$

This is discussed in detail in [6].

2. $\mathbb{Z}_4, \mathbf{A}_1 \times \mathbf{A}_1 \times \mathbf{B}_2 \times \mathbf{B}_2$

Discussed in [6].

3. $\mathbb{Z}_4, \mathbf{A}_1 \times \mathbf{A}_3 \times \mathbf{B}_2$

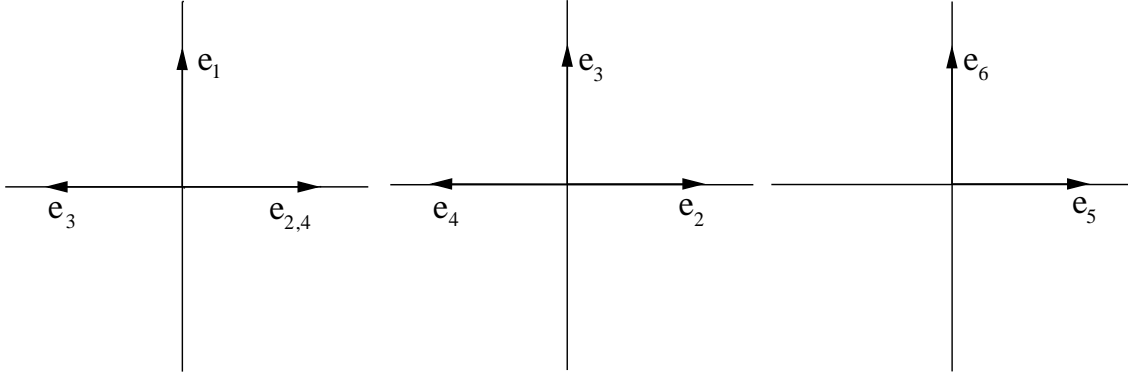


Figure 8: The $\mathbb{Z}_4, \mathbf{A}_1 \times \mathbf{A}_3 \times \mathbf{B}_2$ lattice

$$\begin{aligned} \omega \mathbf{e}_1 &= -\mathbf{e}_1 & \omega \mathbf{e}_2 &= \mathbf{e}_3 & \omega \mathbf{e}_3 &= \mathbf{e}_4 \\ \omega \mathbf{e}_4 &= -\mathbf{e}_2 - \mathbf{e}_3 - \mathbf{e}_4 & \omega \mathbf{e}_5 &= \mathbf{e}_6 & \omega \mathbf{e}_6 &= -\mathbf{e}_5. \end{aligned}$$

$$g_{ij} = \mathbf{e}_i \cdot \mathbf{e}_j = \begin{pmatrix} 1 & 0 & 0 & 0 & 0 & 0 \\ 0 & 1 & -\frac{1}{2} & 0 & 0 & 0 \\ 0 & -\frac{1}{2} & 1 & -\frac{1}{2} & 0 & 0 \\ 0 & 0 & -\frac{1}{2} & 1 & 0 & 0 \\ 0 & 0 & 0 & 0 & 1 & 0 \\ 0 & 0 & 0 & 0 & 0 & 1 \end{pmatrix} \quad (115)$$

$$(\det g)^{\frac{1}{2}} = \frac{1}{\sqrt{2}}. \quad (116)$$

4. $\mathbb{Z}_4, \mathbf{A}_3 \times \mathbf{A}_3$

Discussed in section 5.6.

5. $\mathbb{Z}_6, \mathbf{A}_2 \times \mathbf{G}_2 \times \mathbf{G}_2$

Discussed in [6].

6. $\mathbb{Z}_6, \mathbf{G}_2 \times \mathbf{A}_2 \times \mathbf{A}_2, \Theta = \Gamma_1 \Gamma_2 \Gamma_3 \Gamma_4 P_{36} P_{45}$

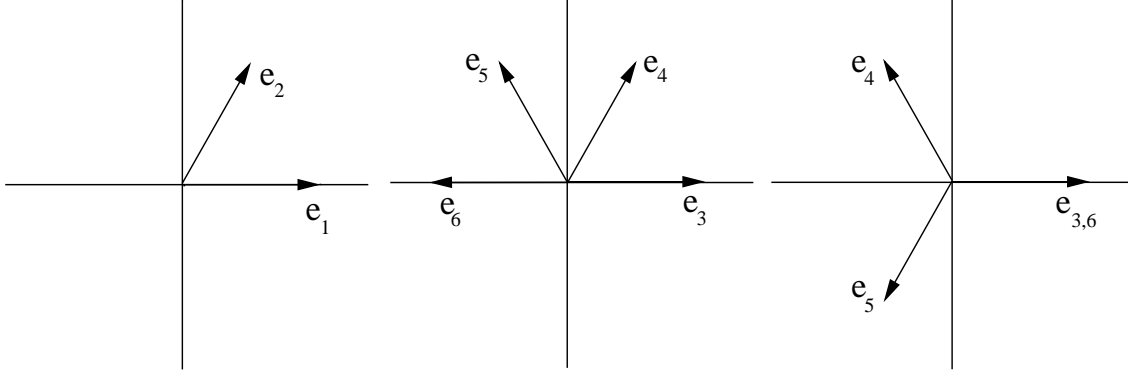


Figure 9: The $\mathbb{Z}_6, G_2 \times A_2 \times A_2$ lattice

$$\begin{aligned} \omega \mathbf{e}_1 &= \mathbf{e}_2 & \omega \mathbf{e}_2 &= -\mathbf{e}_1 + \mathbf{e}_2 & \omega \mathbf{e}_3 &= \mathbf{e}_4 \\ \omega \mathbf{e}_4 &= \mathbf{e}_5 & \omega \mathbf{e}_5 &= \mathbf{e}_6 & \omega \mathbf{e}_6 &= -\mathbf{e}_3 - \mathbf{e}_5. \end{aligned}$$

$$g_{ij} = \mathbf{e}_i \cdot \mathbf{e}_j = \begin{pmatrix} 1 & \frac{1}{2} & 0 & 0 & 0 & 0 \\ \frac{1}{2} & 1 & 0 & 0 & 0 & 0 \\ 0 & 0 & 1 & 0 & -\frac{1}{2} & 0 \\ 0 & 0 & 0 & 1 & 0 & -\frac{1}{2} \\ 0 & 0 & -\frac{1}{2} & 0 & 1 & 0 \\ 0 & 0 & 0 & -\frac{1}{2} & 0 & 1 \end{pmatrix} \quad (117)$$

$$(\det g)^{\frac{1}{2}} = \frac{3\sqrt{3}}{8}. \quad (118)$$

7. $\mathbb{Z}'_6, \mathbf{A}_1 \times \mathbf{A}_1 \times \mathbf{A}_2 \times \mathbf{G}_2$

Discussed in [6].

8. $\mathbb{Z}'_6, \mathbf{A}_2 \times \mathbf{D}_4$

For this orbifold there did not appear to be a natural description in terms of the formalism outlined in section 2.

9. $\mathbb{Z}'_6, \mathbf{A}_1 \times \mathbf{A}_1 \times \mathbf{A}_2 \times \mathbf{A}_2, \Theta = \Gamma_1 \Gamma_2 \Gamma_3 \Gamma_4 P_{36} P_{45}$

$$\begin{aligned} \omega \mathbf{e}_1 &= -\mathbf{e}_1 & \omega \mathbf{e}_2 &= -\mathbf{e}_2 & \omega \mathbf{e}_3 &= \mathbf{e}_4 \\ \omega \mathbf{e}_4 &= \mathbf{e}_5 & \omega \mathbf{e}_5 &= \mathbf{e}_6 & \omega \mathbf{e}_6 &= -\mathbf{e}_3 - \mathbf{e}_5. \end{aligned}$$

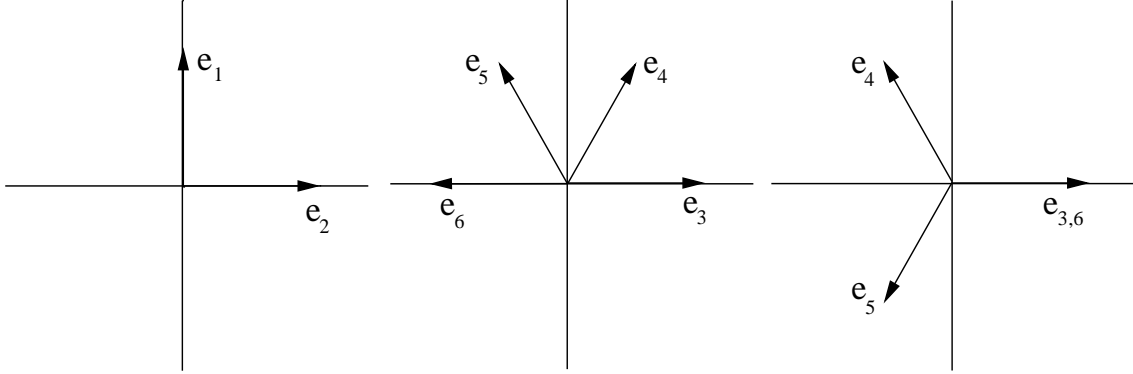


Figure 10: The $\mathbb{Z}'_6, A_1 \times A_1 \times A_2 \times A_2$ lattice

$$g_{ij} = \mathbf{e}_i \cdot \mathbf{e}_j = \begin{pmatrix} 1 & 0 & 0 & 0 & 0 & 0 \\ 0 & 1 & 0 & 0 & 0 & 0 \\ 0 & 0 & 1 & 0 & -\frac{1}{2} & 0 \\ 0 & 0 & 0 & 1 & 0 & -\frac{1}{2} \\ 0 & 0 & -\frac{1}{2} & 0 & 1 & 0 \\ 0 & 0 & 0 & -\frac{1}{2} & 0 & 1 \end{pmatrix} \quad (119)$$

$$(\det g)^{\frac{1}{2}} = \frac{3}{4}. \quad (120)$$

10. $\mathbb{Z}'_6, \mathbf{A}_1 \times \mathbf{A}_5$

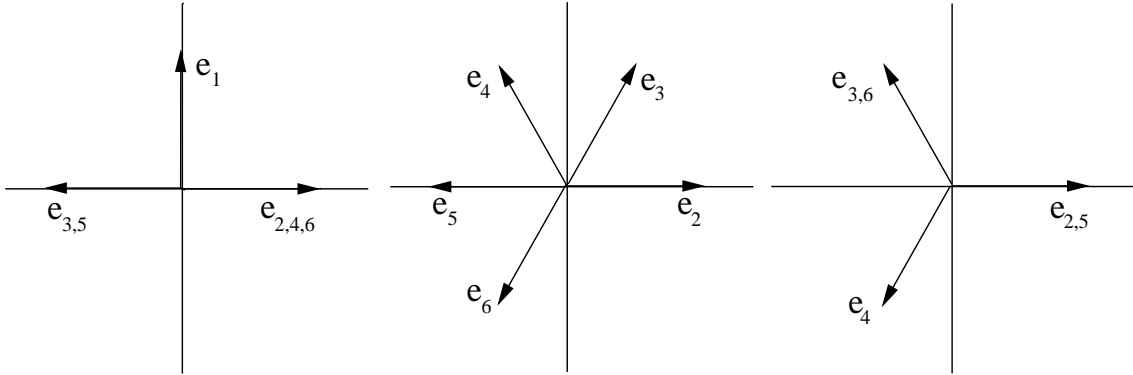


Figure 11: The $\mathbb{Z}'_6, A_1 \times A_5$ lattice

$$\begin{aligned} \omega \mathbf{e}_1 &= -\mathbf{e}_1 & \omega \mathbf{e}_2 &= \mathbf{e}_3 & \omega \mathbf{e}_3 &= \mathbf{e}_4 \\ \omega \mathbf{e}_4 &= \mathbf{e}_5 & \omega \mathbf{e}_5 &= \mathbf{e}_6 & \omega \mathbf{e}_6 &= -\mathbf{e}_2 - \mathbf{e}_3 - \mathbf{e}_4 - \mathbf{e}_5 - \mathbf{e}_6. \end{aligned}$$

$$g_{ij} = \mathbf{e}_i \cdot \mathbf{e}_j = \begin{pmatrix} 1 & 0 & 0 & 0 & 0 & 0 \\ 0 & 1 & -\frac{1}{2} & 0 & 0 & 0 \\ 0 & -\frac{1}{2} & 1 & -\frac{1}{2} & 0 & 0 \\ 0 & 0 & -\frac{1}{2} & 1 & -\frac{1}{2} & 0 \\ 0 & 0 & 0 & -\frac{1}{2} & 1 & -\frac{1}{2} \\ 0 & 0 & 0 & 0 & -\frac{1}{2} & 1 \end{pmatrix} \quad (121)$$

$$(\det g)^{\frac{1}{2}} = \frac{3}{4}. \quad (122)$$

11. $\mathbb{Z}_7, \mathbf{A}_6$

See section 5.1.

12. $\mathbb{Z}_8, \mathbf{B}_4 \times \mathbf{D}_2$

See section 5.3.

13. $\mathbb{Z}_8, \mathbf{A}_1 \times \mathbf{D}_5$

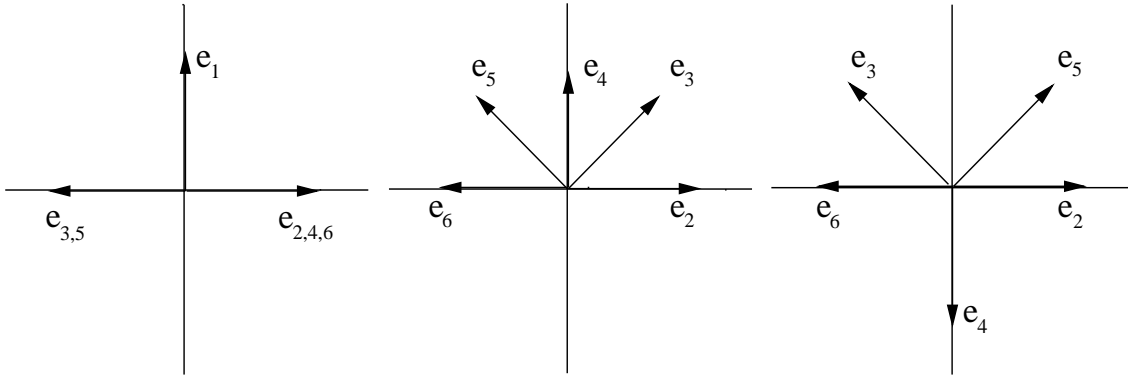


Figure 12: The $\mathbb{Z}_8, \mathbf{A}_1 \times \mathbf{D}_5$ lattice

$$\begin{aligned} \omega \mathbf{e}_1 &= -\mathbf{e}_1 & \omega \mathbf{e}_2 &= \mathbf{e}_3 & \omega \mathbf{e}_3 &= \mathbf{e}_4 \\ \omega \mathbf{e}_4 &= \mathbf{e}_5 & \omega \mathbf{e}_5 &= \mathbf{e}_6 & \omega \mathbf{e}_6 &= -\mathbf{e}_2 - \mathbf{e}_3 - \mathbf{e}_6. \end{aligned}$$

$$g_{ij} = \mathbf{e}_i \cdot \mathbf{e}_j = \begin{pmatrix} 1 & 0 & 0 & 0 & 0 & 0 \\ 0 & 1 & -\frac{1}{2} & \frac{1}{2} & -\frac{1}{2} & 0 \\ 0 & -\frac{1}{2} & 1 & -\frac{1}{2} & \frac{1}{2} & -\frac{1}{2} \\ 0 & \frac{1}{2} & -\frac{1}{2} & 1 & -\frac{1}{2} & \frac{1}{2} \\ 0 & -\frac{1}{2} & \frac{1}{2} & -\frac{1}{2} & 1 & -\frac{1}{2} \\ 0 & 0 & -\frac{1}{2} & \frac{1}{2} & -\frac{1}{2} & 1 \end{pmatrix} \quad (123)$$

$$(\det g)^{\frac{1}{2}} = \frac{1}{2\sqrt{2}}. \quad (124)$$

14. $\mathbb{Z}'_8, \mathbf{B}_2 \times \mathbf{B}_4$

See section 5.2.

15. $\mathbb{Z}'_8, \mathbf{A}_3 \times \mathbf{A}_3, \Theta = \Gamma_1 \Gamma_2 \Gamma_3 P_{16} P_{25} P_{34}$

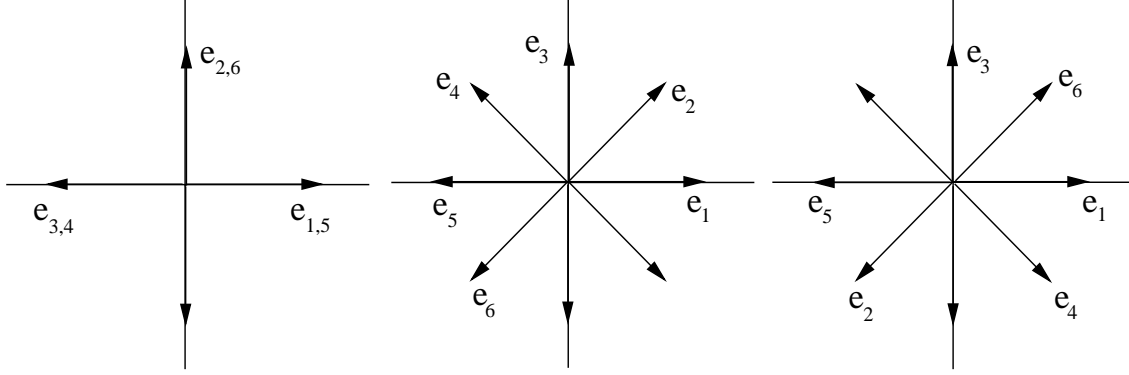


Figure 13: The $\mathbb{Z}'_8, A_3 \times A_3$ lattice

$$\begin{aligned} \omega \mathbf{e}_1 &= \mathbf{e}_2 & \omega \mathbf{e}_2 &= \mathbf{e}_3 & \omega \mathbf{e}_3 &= \mathbf{e}_4 \\ \omega \mathbf{e}_4 &= \mathbf{e}_5 & \omega \mathbf{e}_5 &= \mathbf{e}_6 & \omega \mathbf{e}_6 &= -\mathbf{e}_1 - \mathbf{e}_3 - \mathbf{e}_5. \end{aligned}$$

$$g_{ij} = \mathbf{e}_i \cdot \mathbf{e}_j = \begin{pmatrix} 1 & 0 & -\frac{1}{2} & 0 & 0 & 0 \\ 0 & 1 & 0 & -\frac{1}{2} & 0 & 0 \\ -\frac{1}{2} & 0 & 1 & 0 & -\frac{1}{2} & 0 \\ 0 & -\frac{1}{2} & 0 & 1 & 0 & -\frac{1}{2} \\ 0 & 0 & -\frac{1}{2} & 0 & 1 & 0 \\ 0 & 0 & 0 & -\frac{1}{2} & 0 & 1 \end{pmatrix} \quad (125)$$

$$(\det g)^{\frac{1}{2}} = \frac{1}{2}. \quad (126)$$

16. $\mathbb{Z}_{12}, \mathbf{A}_2 \times \mathbf{F}_4$

See section 5.4.

17. $\mathbb{Z}_{12}, \mathbf{E}_6$

$$\begin{aligned} \omega \mathbf{e}_1 &= \mathbf{e}_2, & \omega \mathbf{e}_2 &= \mathbf{e}_3, & \omega \mathbf{e}_3 &= \mathbf{e}_4 \\ \omega \mathbf{e}_4 &= \mathbf{e}_5, & \omega \mathbf{e}_5 &= \mathbf{e}_6, & \omega \mathbf{e}_6 &= \mathbf{e}_4 - \mathbf{e}_1 - \mathbf{e}_2 - \mathbf{e}_6. \end{aligned}$$

$$g_{ij} = \mathbf{e}_i \cdot \mathbf{e}_j = \begin{pmatrix} 1 & -\frac{1}{2} & 0 & \frac{1}{2} & -\frac{1}{2} & 0 \\ -\frac{1}{2} & 1 & -\frac{1}{2} & 0 & \frac{1}{2} & -\frac{1}{2} \\ 0 & -\frac{1}{2} & 1 & -\frac{1}{2} & 0 & \frac{1}{2} \\ \frac{1}{2} & 0 & -\frac{1}{2} & 1 & -\frac{1}{2} & 0 \\ -\frac{1}{2} & \frac{1}{2} & 0 & -\frac{1}{2} & 1 & -\frac{1}{2} \\ 0 & -\frac{1}{2} & \frac{1}{2} & 0 & -\frac{1}{2} & 1 \end{pmatrix} \quad (127)$$

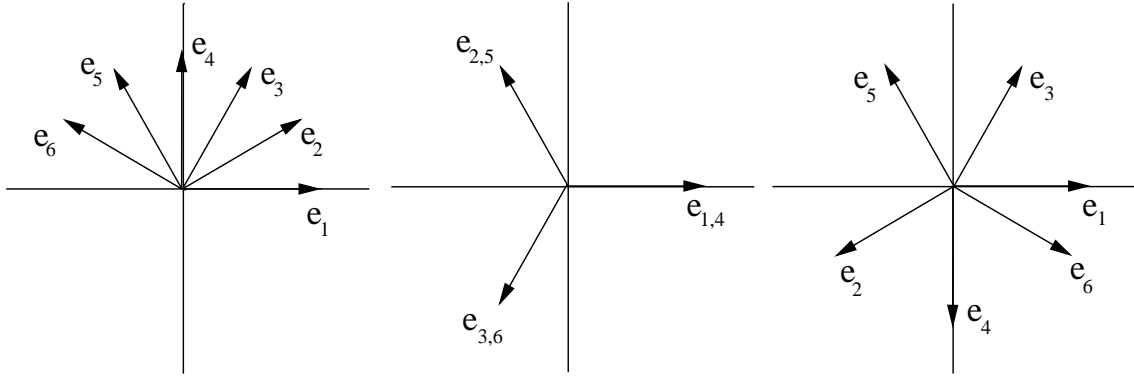


Figure 14: The \mathbb{Z}_{12}, E_6 lattice

$$(\det g)^{\frac{1}{2}} = \frac{\sqrt{3}}{8}. \quad (128)$$

18. $\mathbb{Z}'_{12}, \mathbf{D}_2 \times \mathbf{F}_4$
See section 5.5.

References

- [1] C. Angelantonj and A. Sagnotti, “Open Strings,” *Phys. Rept.* **371** (2002) 1–150, [hep-th/0204089](#).
- [2] C. Bachas, “A Way to Break Supersymmetry,” [hep-th/9503030](#).
- [3] M. Berkooz, M. R. Douglas, and R. G. Leigh, “Branes Intersecting at Angles,” *Nucl. Phys.* **B480** (1996) 265–278, [hep-th/9606139](#).
- [4] R. Blumenhagen, L. Görlich, and B. Körs, “Supersymmetric orientifolds in 6D with D-branes at angles,” *Nucl. Phys.* **B569** (2000) 209–228, [hep-th/9908130](#).
- [5] C. Angelantonj and R. Blumenhagen, “Discrete deformations in type I vacua,” *Phys. Lett.* **B473** (2000) 86–93, [hep-th/9911190](#).
- [6] R. Blumenhagen, L. Görlich, and B. Körs, “Supersymmetric 4D orientifolds of type IIA with D6-branes at angles,” *JHEP* **01** (2000) 040, [hep-th/9912204](#).
- [7] G. Pradisi, “Type I vacua from diagonal \mathbb{Z}_3 -orbifolds,” *Nucl. Phys.* **B575** (2000) 134–150, [hep-th/9912218](#).
- [8] S. Förste, G. Honecker, and R. Schreyer, “Supersymmetric $\mathbb{Z}_N \times \mathbb{Z}_M$ orientifolds in 4D with D-branes at angles,” *Nucl. Phys.* **B593** (2001) 127–154, [hep-th/0008250](#).
- [9] R. Blumenhagen, L. Görlich, B. Körs, and D. Lüst, “Asymmetric orbifolds, noncommutative geometry and type I string vacua,” *Nucl. Phys.* **B582** (2000) 44–64, [hep-th/0003024](#).
- [10] R. Blumenhagen, L. Görlich, B. Körs, and D. Lüst, “Noncommutative Compactifications of Type I Strings on Tori with Magnetic Background Flux,” *JHEP* **10** (2000) 006, [hep-th/0007024](#).
- [11] C. Angelantonj, I. Antoniadis, E. Dudas, and A. Sagnotti, “Type-I strings on magnetised orbifolds and brane transmutation,” *Phys. Lett.* **B489** (2000) 223–232, [hep-th/0007090](#).
- [12] G. Aldazabal, S. Franco, L. E. Ibanez, R. Rabadan, and A. M. Uranga, “Intersecting brane worlds,” *JHEP* **02** (2001) 047, [hep-ph/0011132](#).
- [13] G. Aldazabal, S. Franco, L. E. Ibanez, R. Rabadan, and A. M. Uranga, “D = 4 Chiral String Compactifications from Intersecting Branes,” *J. Math. Phys.* **42** (2001) 3103–3126, [hep-th/0011073](#).

- [14] R. Blumenhagen, B. K rs, and D. L st, “Type I strings with F- and B-flux,” *JHEP* **02** (2001) 030, [hep-th/0012156](#).
- [15] L. E. Ibanez, F. Marchesano, and R. Rabadan, “Getting just the standard model at intersecting branes,” *JHEP* **11** (2001) 002, [hep-th/0105155](#).
- [16] R. Blumenhagen, B. K rs, D. L st, and T. Ott, “The Standard Model from Stable Intersecting Brane World Orbifolds,” *Nucl. Phys.* **B616** (2001) 3–33, [hep-th/0107138](#).
- [17] D. Bailin, G. V. Kraniotis, and A. Love, “Standard-like models from intersecting D4-branes,” *Phys. Lett.* **B530** (2002) 202–209, [hep-th/0108131](#).
- [18] C. Kokorelis, “GUT model hierarchies from intersecting branes,” *JHEP* **08** (2002) 018, [hep-th/0203187](#).
- [19] M. Cvetič, G. Shiu, and A. M. Uranga, “Three-family supersymmetric standard like models from intersecting brane worlds,” *Phys. Rev. Lett.* **87** (2001) 201801, [hep-th/0107143](#).
- [20] M. Cvetič, G. Shiu, and A. M. Uranga, “Chiral four-dimensional $N = 1$ supersymmetric type IIA orientifolds from intersecting D6-branes,” *Nucl. Phys.* **B615** (2001) 3–32, [hep-th/0107166](#).
- [21] R. Blumenhagen, L. G rlich, and T. Ott, “Supersymmetric intersecting branes on the type IIA T^6/\mathbb{Z}_4 orientifold,” *JHEP* **01** (2003) 021, [hep-th/0211059](#).
- [22] G. Honecker, “Chiral supersymmetric models on an orientifold of $\mathbb{Z}_4 \times \mathbb{Z}_2$ with intersecting D6-branes,” *Nucl. Phys.* **B666** (2003) 175–196, [hep-th/0303015](#).
- [23] M. Cvetič and I. Papadimitriou, “More supersymmetric standard-like models from intersecting D6-branes on type IIA orientifolds,” *Phys. Rev.* **D67** (2003) 126006, [hep-th/0303197](#).
- [24] T.-j. Li and T. Liu, “Supersymmetric G^3 unification from intersecting D6-branes on type IIA orientifolds,” *Phys. Lett.* **B573** (2003) 193–201, [hep-th/0304258](#).
- [25] M. Larosa and G. Pradisi, “Magnetized four-dimensional $\mathbb{Z}_2 \times \mathbb{Z}_2$ orientifolds,” *Nucl. Phys.* **B667** (2003) 261–309, [hep-th/0305224](#).
- [26] G. Honecker and T. Ott, “Getting just the Supersymmetric Standard Model at Intersecting Branes on the \mathbb{Z}_6 -orientifold,” [hep-th/0404055](#).

- [27] M. Cvetič, T. Li, and T. Liu, “Supersymmetric Pati-Salam models from intersecting D6- branes: A road to the standard model,” [hep-th/0403061](#).
- [28] A. M. Uranga, “Chiral four-dimensional string compactifications with intersecting D-branes,” *Class. Quant. Grav.* **20** (2003) S373–S394, [hep-th/0301032](#).
- [29] D. Lüst, “Intersecting Brane Worlds: A Path to the Standard Model?,” [hep-th/0401156](#).
- [30] C. Angelantonj, M. Bianchi, G. Pradisi, A. Sagnotti, and Y. S. Stanev, “Comments on Gepner models and type I vacua in string theory,” *Phys. Lett.* **B387** (1996) 743–749, [hep-th/9607229](#).
- [31] R. Blumenhagen and A. Wisskirchen, “Spectra of 4D, $N = 1$ type I string vacua on non-toroidal CY threefolds,” *Phys. Lett.* **B438** (1998) 52–60, [hep-th/9806131](#).
- [32] G. Aldazabal, E. C. Andres, M. Leston, and C. Nunez, “Type IIB orientifolds on Gepner points,” *JHEP* **09** (2003) 067, [hep-th/0307183](#).
- [33] R. Blumenhagen, “Supersymmetric orientifolds of Gepner models,” *JHEP* **11** (2003) 055, [hep-th/0310244](#).
- [34] I. Brunner, K. Hori, K. Hosomichi, and J. Walcher, “Orientifolds of Gepner models,” [hep-th/0401137](#).
- [35] R. Blumenhagen and T. Weigand, “Chiral supersymmetric Gepner model orientifolds,” *JHEP* **02** (2004) 041, [hep-th/0401148](#).
- [36] T. P. T. Dijkstra, L. R. Huiszoon, and A. N. Schellekens, “Chiral supersymmetric standard model spectra from orientifolds of Gepner models,” [hep-th/0403196](#).
- [37] R. Blumenhagen and T. Weigand, “A note on partition functions of Gepner model orientifolds,” [hep-th/0403299](#).
- [38] G. Aldazabal, E. C. Andres, and J. E. Juknevich, “Particle models from orientifolds at Gepner-orbifold points,” [hep-th/0403262](#).
- [39] Z. Kakushadze and G. Shiu, “A chiral $N = 1$ type I vacuum in four dimensions and its heterotic dual,” *Phys. Rev.* **D56** (1997) 3686–3697, [hep-th/9705163](#).
- [40] G. Aldazabal, A. Font, L. E. Ibanez, and G. Violero, “ $D = 4$, $N = 1$, type IIB orientifolds,” *Nucl. Phys.* **B536** (1998) 29–68, [hep-th/9804026](#).

- [41] G. Zwart, “Four-dimensional $N = 1$ $Z(N) \times Z(M)$ orientifolds,” *Nucl. Phys.* **B526** (1998) 378–392, [hep-th/9708040](#).
- [42] Z. Kakushadze, G. Shiu, and S. H. H. Tye, “Type IIB orientifolds, F-theory, type I strings on orbifolds and type I heterotic duality,” *Nucl. Phys.* **B533** (1998) 25–87, [hep-th/9804092](#).
- [43] M. R. Gaberdiel, “Lectures on non-BPS Dirichlet branes,” *Class. Quant. Grav.* **17** (2000) 3483–3520, [hep-th/0005029](#).
- [44] L. J. Dixon, J. A. Harvey, C. Vafa, and E. Witten, “Strings on Orbifolds,” *Nucl. Phys.* **B261** (1985) 678–686.
- [45] L. J. Dixon, J. A. Harvey, C. Vafa, and E. Witten, “Strings on Orbifolds(II),” *Nucl. Phys.* **B274** (1986) 285–314.
- [46] J. Erler and A. Klemm, “Comment on the Generation Number in Orbifold Compactifications,” *Commun. Math. Phys.* **153** (1993) 579–604, [hep-th/9207111](#).
- [47] R. Blumenhagen, V. Braun, B. Körs, and D. Lüst, “Orientifolds of K3 and Calabi-Yau manifolds with intersecting D-branes,” *JHEP* **07** (2002) 026, [hep-th/0206038](#).
- [48] J. A. Casas, F. Gomez, and C. Munoz, “Complete structure of \mathbb{Z}_n Yukawa couplings,” *Int. J. Mod. Phys.* **A8** (1993) 455–506, [hep-th/9110060](#).
- [49] M. Klein and R. Rabadan, “D = 4, N = 1 orientifolds with vector structure,” *Nucl. Phys.* **B596** (2001) 197–230, [hep-th/0007087](#).
- [50] E. G. Gimon and J. Polchinski, “Consistency Conditions for Orientifolds and D-Manifolds,” *Phys. Rev.* **D54** (1996) 1667–1676, [hep-th/9601038](#).
- [51] A. Dabholkar, “Lectures on Orientifolds and Duality,” [hep-th/9804208](#).
- [52] S. Kachru and J. McGreevy, “M-theory on manifolds of G(2) holonomy and type IIA orientifolds,” *JHEP* **06** (2001) 027, [hep-th/0103223](#).
- [53] M. Atiyah and E. Witten, “M-theory dynamics on a manifold of G(2) holonomy,” *Adv. Theor. Math. Phys.* **6** (2003) 1–106, [hep-th/0107177](#).
- [54] E. Witten, “Anomaly cancellation on G(2) manifolds,” [hep-th/0108165](#).
- [55] D. Cremades, L. E. Ibanez, and F. Marchesano, “Yukawa couplings in intersecting D-brane models,” *JHEP* **07** (2003) 038, [hep-th/0302105](#).
- [56] D. Lüst and S. Stieberger, “Gauge threshold corrections in intersecting brane world models,” [hep-th/0302221](#).

- [57] M. Cvetič and I. Papadimitriou, “Conformal field theory couplings for intersecting D-branes on orientifolds,” *Phys. Rev.* **D68** (2003) 046001, [hep-th/0303083](#).
- [58] S. A. Abel and A. W. Owen, “Interactions in intersecting brane models,” *Nucl. Phys.* **B663** (2003) 197–214, [hep-th/0303124](#).
- [59] S. A. Abel and A. W. Owen, “N-point amplitudes in intersecting brane models,” [hep-th/0310257](#).
- [60] B. K rs and P. Nath, “Effective action and soft supersymmetry breaking for intersecting D-brane models,” *Nucl. Phys.* **B681** (2004) 77–119, [hep-th/0309167](#).
- [61] D. L st, P. Mayr, R. Richter, and S. Stieberger, “Scattering of Gauge, Matter, and Moduli Fields from Intersecting Branes,” [hep-th/0404134](#).
- [62] D. Cremades, L. E. Ibanez, and F. Marchesano, “Computing Yukawa Couplings from Magnetized Extra Dimensions,” [hep-th/0404229](#).